# Discovery of a Novel Alpha-7 Nicotinic Acetylcholine Receptor Agonist Series and Characterization of the Potent, Selective, and Orally Efficacious Agonist 5-(4-Acetyl[1,4]diazepan-1-yl)pentanoic Acid [5-(4-Methoxyphenyl)-1H-pyrazol-3-yl] Amide (SEN15924, WAY-361789)

Riccardo Zanaletti,*,[†] Laura Bettinetti,[†] Cristiana Castaldo,[†] Giuseppe Cocconcelli,[†] Thomas Comery,[‡] John Dunlop,[‡] Giovanni Gaviraghi,[†] Chiara Ghiron,[†] Simon N. Haydar,[‡] Flora Jow,[‡] Laura Maccari,[†] Iolanda Micco,[†] Arianna Nencini,[†] Carla Scali,[†] Elisa Turlizzi,[†] and Michela Valacchi[†]

[†]Siena Biotech SpA, Strada del Petriccio e Belriguardo 35, 53100 Siena, Italy

[‡]Neuroscience Research Unit, Pfizer, Eastern Point Road, Groton Connecticut 06340, United States

ABSTRACT: Alpha-7 nicotinic acetylcholine receptors (α7 nAChR) are implicated in the modulation of many cognitive functions such as attention, working memory, and episodic memory. For this reason, α7 nAChR agonists represent promising therapeutic candidates for the treatment of cognitive impairment associated with Alzheimer's disease (AD) and schizophrenia. A medicinal chemistry effort, around our previously reported chemical series, permitted the discovery of a novel class of α7 nAChR agonists with improved selectivity, in particular against the α3 receptor subtype and better ADME profile. The exploration of this series led to the identification of 5-(4-acetyl[1,4]diazepan-1-yl)pentanoic acid [5-(4-methoxyphenyl)-1H-pyrazol-3-yl] amide (**25**, SEN15924, WAY-361789), a novel, full agonist of the α7 nAChR that was evaluated *in vitro* and *in vivo*. Compound **25** proved to be potent and selective, and it demonstrated a fair pharmacokinetic profile accompanied by efficacy in rodent behavioral cognition models (novel object recognition and auditory sensory gating).
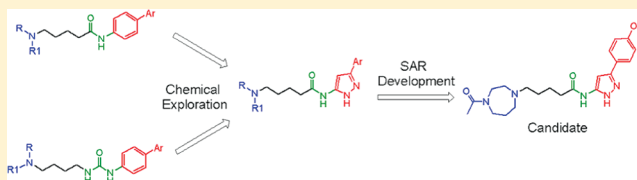
■ INTRODUCTION

Schizophrenia and Alzheimer's disease are both chronic conditions characterized by dramatic and debilitating symptoms. Schizophrenia typically occurs in young adulthood, with a prevalence of about 1.0% of the population,[1] and is characterized by positive and negative symptoms (hallucinations, delusions, reduced affect, social withdrawal, low motivation, disorganized thoughts) and cognitive impairment (decreased attention, memory deficits). While positive symptoms are partially managed with current medications, cognitive deficits and negative symptoms still remain an unmet medical need.

Alzheimer's disease is most often diagnosed in people over 65 years of age in industrialized countries,[2] although early onset disease can occur much earlier. In 2006, 26.6 million people suffered worldwide from this condition, and by 2050, 1 in 85 people globally is expected to be affected, with the consequent economic burden predicted to be unbearable.[3] In Alzheimer's disease, only modest, temporary, and symptomatic improvement in cognitive performance is provided by standard of care agents such as acetylcholinesterase inhibitors and 3,5-dimethyladamantan-1-ylamine (memantine, a NMDA receptor antagonist).

Neuronal nicotinic acetylcholine receptors are a family of ligand gated ion channels permeable to cations such as Na$^+$, K$^+$,

and Ca^{2+}. nAChRs are pentameric combinations of five subunits that can assemble as homopentamers or heteropentamers of 12 distinct subunits (α2-α10, β2-β4).

The homomeric α7 nACh receptor is one of the most abundant nicotinic receptors in the human brain and is highly expressed in regions associated with learning and memory such as the cerebral cortex and the hippocampus. This receptor, compared to other nicotinic receptors, activates and desensitizes rapidly upon agonist binding, is more permeable to calcium, and is less sensitive to ACh and nicotine.[4,5]

The link between α7 nAChR and cognition is not completely understood but has been associated with the high Ca^{2+} permeability of this receptor. This is responsible for modulating neurotransmitter pathways and for the activation of biochemical signaling pathways, including phosphorylated extracellular-regulated kinase (pERK) and phosphorylated cAMP response element binding protein (pCREB).[6,7] The phosphorylation of CREB can increase the transcription of various genes that may be responsible for long-lasting effects on synaptic plasticity and memory.[8]

Several lines of experimental evidence support the involvement of the α7 neuronal nAChR in both schizophrenia

and AD.[9−12] These include reduced expression of α7 nAChR in brain tissue from schizophrenia and AD patients, as well as genetic linkage studies in schizophrenia, implicating the locus of the α7 receptor gene promoter.[13] Prototypical α7 nAChR agonists have demonstrated improved cognition in animal models and normalized sensory gating deficits, which are believed to contribute to the cognitive fragmentation in schizophrenia.[14,15]

On the basis of these observations, there is strong hope that selective α7 nAChR agonists will prove effective in the improvement of cognition in both schizophrenia and AD.[16−18] In accordance with this hypothesis, the prototypical nAChR agonist nicotine, as well as more selective α7 agonists described recently, have been shown to ameliorate cognitive performance in both animal models and human clinical trials. In the past decade, there has been a continuous effort to develop new α7 nAChR agonists with better properties, and many of them have advanced into clinical trials. Some examples are reported in Figure 1: EVP-6124 and TC-5619, which are
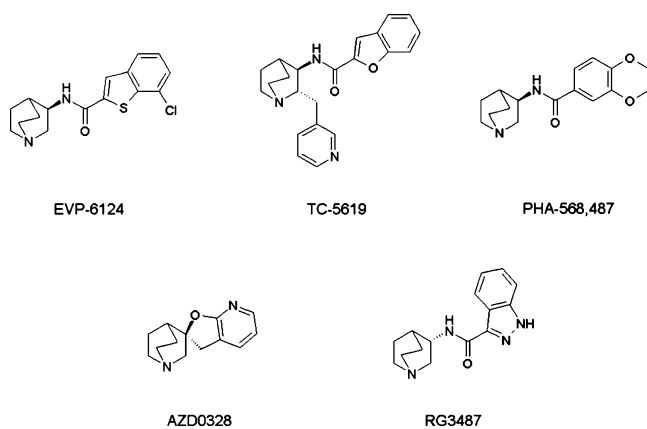

Figure 1. α7 nAChR ligands evaluated in the clinical phase.

currently in phase 2 studies for schizophrenia and Alzheimer's disease, are well tolerated and have shown efficacy outcomes; PHA568,487 was discontinued for cardiovascular findings of nonsustained ventricular tachycardia in humans, while AZD0328 and RG3487 did not meet the desired target product profile in phase 2. As highlighted in Figure 1, most of the α7 agonists reported to date belong to the quinuclidine family and the efforts to design different scaffolds have mainly led to bicyclic amine compounds (Figure 2).[19]
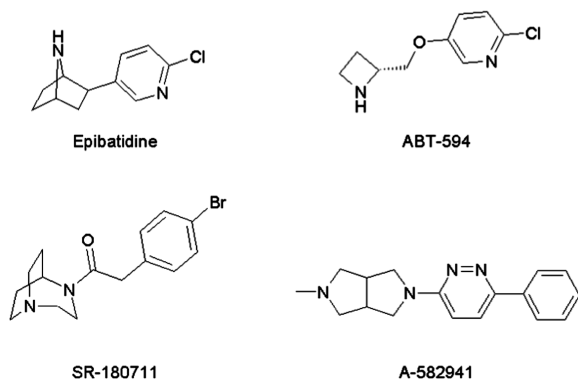

Figure 2. Nonquinuclidine amine templates in the nAChR field.

The traditional pharmacophore model for α7 agonists includes a core cationic center and a hydrogen bond acceptor,[20,21] as exemplified by nicotine, acetylcholine, and epibatidine. This two-point interaction model has been confirmed by several X-ray cocrystal structures of α7 agonists bound to the homopentameric acetylcholine binding protein (AChBP). AChBP is a structural homologue of the α7 agonist binding domain and, in the absence of the α7 crystal structure, is widely used as a surrogate of nicotinic receptors and as a template to build theoretical receptor models.[22] The agonist binding site is located at the monomer interfaces and is mostly buried by the Cys-loop, which delimits the site together with an aromatic cage composed of W53, Y89, W143, Y164, Y185, and Y192. The core pharmacophoric interaction occurs between the basic center of the ligand and W143 of the aromatic cage via a cation-π or hydrogen bonding contact; many cocrystal structures also show a well-conserved water molecule that establishes a hydrogen bond with the agonist, as in the case of nicotine.[23]

We have previously reported[24,25] two chemical series of α7 agonists (series 1 and 2, Figure 3). Both are characterized by
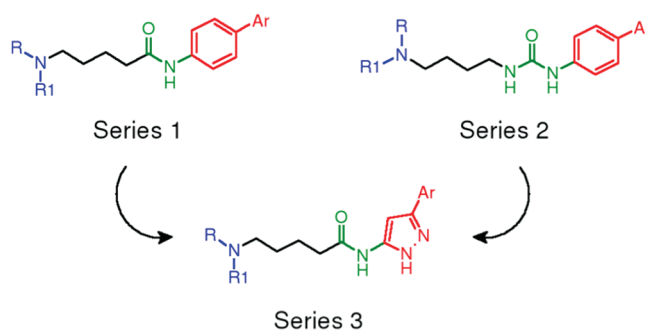

Figure 3. Series 1, 2, 3 and pharmacophoric features: basic center (blue); carbon chain (black); central linker (green); and biaryl system (red).

the presence of a basic center, which is the key pharmacophoric feature, together with a linear four carbon chain, a central linker, and a biaryl system, typical of our series. The key difference between the two series is the central linker: an amide group for series 1; a urea moiety for series 2.

Series 2 shows generally better potency against α7 nAChR compared to series 1; both suffer from low selectivity, particularly against the homologous ganglionic α3 receptor. Series 2 is also characterized by a nonoptimal hERG activity and substantial cytochrome inhibition. We aimed at developing a new series that combines good potency and selectivity with no hERG and cytochrome inhibition and with the final purpose of developing a potential preclinical candidate. Our medicinal chemistry effort focused on exploring the first ring of the biaryl system in series 1 and led us to the discovery of series 3. Series 3 shows a good level of potency, better selectivity, an optimal hERG profile, and no cytochrome P450 inhibition. Interestingly, series 3 retains two hydrogen bond donors, thus the possibility of an extra interaction, compared to series 2. Molecular modeling studies were also applied to investigate the structural basis of ligand−receptor binding and to define the pharmacophoric features of the described α7 nAChR agonists. Herein we report the synthesis, SAR development, pharmacological characterization, and the *in vivo* efficacy of this novel series of α7 nAChR agonists.

Table 1. Effect of First Ring Replacement on Activity

Compound	Structure	α7 EC$_{50}$ (μM) ± SEM (n)[a]	α7 E$_{max}$ (%) ± SEM (n)[a]
1		1.22 ± 0.46 (2)	83 ± 14.6 (2)
2		0.78 ± 0.40 (2)	73 ± 10.8 (2)
3		2.13 ± 0.87 (2)	135 ± 18.2 (2)
4		> Highest Conc (2)	NA (2)
5		2.33 ± 0.62 (2)	56 ± 0.4 (2)
6		> Highest Conc (2)	NA (2)
7		> Highest Conc (2)	NA (2)

[a]All functional activities were measured in a calcium flux assay using a fluorescence imaging plate reader. The activity at rat α7-nAChRs was determined using a stable recombinant GH4C1 cell line expressing the receptor.[35] Reported EC$_{50}$/IC$_{50}$ values were determined in a single experiment and obtained from triplicate data points generated within the same experimental session. Data were averaged from multiple experiments (n) and reported as the average ± SEM (n). Nicotine under the same conditions had EC$_{50}$ = 1.34 μM ± 0.002, E$_{max}$ = 102% ± 1.3 (n = 62), acetylcholine EC$_{50}$ = 3.12 μM ± 0.13, E$_{max}$ = 110% ± 4.1 (n = 6), PHA568,487 EC$_{50}$ = 0.0362 μM ± 0.0006, E$_{max}$ = 96% ± 1.9 (n = 2).

■ RESULTS AND DISCUSSIONS

The initial chemistry effort concentrated on the exploration of the first ring of the biaryl system of series 1, as shown in Table 1. Starting from compound **1** (representative of series 1), we replaced the first phenyl ring with 5-membered heterocycles.

The first objective of this modification was to identify a novel chemical series with acceptable potency and a full functional response. Upon identification of the best heterocycle, the idea was to expand the series to evaluate its potential in terms of activity, selectivity, and ADME profiling data. As appears from the data in Table 1, replacing the phenyl ring of compound **1** with pyrazole gave **3**, with a good level of potency and a full functional response. All the other heterocycles yielded inactive compounds. In the case of **5**, the activity was in the micromolar range but the functional response was only partial; thus, the compound did not further progress. Interestingly, the N-methylated analogue (**4**) of compound **3** was completely inactive, highlighting the importance of the hydrogen bond donor in this position.

Previously reported docking studies[25] have highlighted the putative key interaction pattern of series 2 into a homology model for the human α7 receptor (yellow structure in Figure 4). The piperidine basic nitrogen was engaged in a hydrogen bond interaction with the backbone carbonyl of W143, while the urea moiety was placed within the aromatic cage and stacks over Y89. Moreover, the two NH groups were available to further hydrogen bond to the hydroxyl oxygen of Y185. The four carbon chain acts as a spacer between the two pharmacophoric elements. The terminal part of the biaryl system fits into a polar pocket of the receptor which can establish hydrogen bonding contacts with ligand acceptor atoms. Compound **3** was predicted to have the same interaction pattern (pink structure in Figure 4). Interestingly, the amidic-pyrazole system of **3** was able to mimic the double H-bonding system of the urea series with the two NHs pointing toward
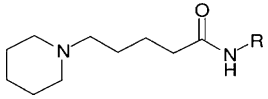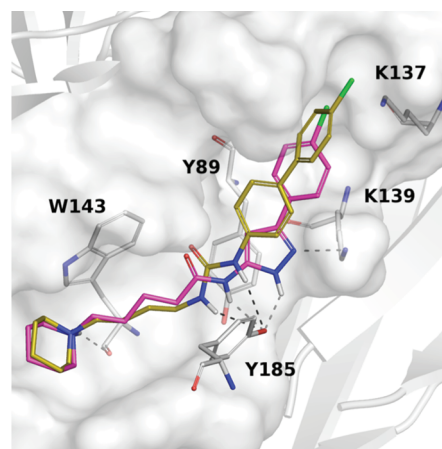

Figure 4. Compounds **2** (yellow) and **3** (pink) bound to the orthosteric site of the theoretical model of human α7 nAChR as predicted by molecular docking studies. Residues involved in key interactions with the ligands are reported. For the sake of clarity, part of the Cys-loop has been removed from the image.

Y185. This conformation is stabilized by an additional hydrogen bond to the protein with respect to the alternative arrangement, proposed by docking calculations, where the two NHs are rotated by 180° and form an intramolecular hydrogen bond. While being energetically favored, such an alternative conformation did not fit to the overall SAR of the series, leading us to prefer the first solution. In this case, the molecule is oriented in order to engage both the double hydrogen bonding system to Y185 and an additional interaction for the hydrogen bond acceptor nitrogen of the pyrazole ring, as described later in the text. The methylation of the pyrazole nitrogen leads to the disruption of the productive contact to Y185 that, together with a steric hindrance effect, makes compound **4** inactive.

Table 2. ClogP, MPSA, Activity, Selectivity (EC$_{50}$ for Agonist Behavior, IC$_{50}$ for Antagonist Behavior), Solubility, Permeability (Perm Class), Metabolic Stability (% Remaining), and P450 Subtype Percent Inhibition at 3 μM, for a Representative Selection of Phenyl Pyrazole Derivatives in Which the Biaryl System Is Explored

Compound	R	ClogP	MPSA (Å^2)	Activity[a] EC$_{50}$ α7 (μM) ± SEM (n)	Selectivity[a] IC$_{50}$ (μM)			Sol[b] (μM)	Perm[c]	Met Stab[d] (%)	P450 inhibition[e] (%)		
					α1	α3	5HT3				3A4	2D6	2C9
3		4.6	61.0	2.13 ± 0.87 (2)	NT	NT	NT	182	High	100	4	11	-3
8		3.9	70.3	0.43 ± 0.12 (3)	>30	3.3	>30	219	High	99	-5	4	-1
9		3.9	70.3	1.70 ± 0.07 (4)	NT	NT	NT	213	High	100	4	-3	-10
10		3.9	70.3	1.45 ± 0.96 (2)	>30	6.4	>30	178	High	100	-34	-2	-7
11		4.1	70.3	3.16 ± 0.06 (2)	NT	NT	NT	188	High	100	-8	4	-9
12		4.1	61.0	1.52 ± 0.53 (2)	>30	3.9	>30	237	High	90	-7	-3	-33
13		4.8	61.0	1.15 ± 0.22 (2)	>30	5.8	>30	144	High	100	9	11	-25
14		2.6	73.9	6.22 ± 0.37 (2)	NT	NT	NT	226	Medium	90	-3	47	-10
15		4.8	61.0	3.07 ± 0.66 (2)	NT	NT	NT	157	High	89	3	13	11
16		3.3	74.2	4.18 ± 0.21 (2)	NT	NT	NT	250	High	92	-6	-5	-33

[a]All functional activities were measured in either calcium flux or membrane potential assays using a fluorescence imaging plate reader. Compounds with E_{max} > 70% of nicotine were considered to be full agonists. The reported compounds gave values >90%. Only compounds with α7 activity lower than 1.5 μM were considered suitable for the selectivity evaluation. NT indicates not tested. [b]Solubilities were determined at pH 7.4 at pseudothermodynamic equilibrium. [c]Permeability was based on measuring the permeation rate of the test article through an artificial membrane. The PAMPA assay uses a mixture of porcine brain lipids in dodecane (2% w/v).[40] [d]Metabolic stability was determined as percentage remaining after incubation for 1 h with recombinant hCYP3A4. [e]Percent cytochrome inhibition values <15−20% were considered low. See Experimental Section for further details on all assays.

Compound **3** was considered a promising starting point to begin an SAR exploration. A representative set of the molecules synthesized is shown in Table 2, with their α7 activity, selectivity over homologous receptor subtypes, and early profiling data.
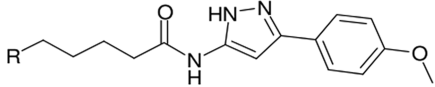
The selection of Table 2 aims to explore the effects of ring substitution in terms of steric hindrance, torsional angle of the biaryl system, and electronic effects on the aromatic rings. The data reported in Table 2 shows that in general the modification of the second ring of the biaryl system has no dramatic impact on α7 activity. Modest loss of potency, compared to our starting molecule (compound **3**), was observed in compounds **14** and **15**, bearing the most electron poor rings. On the contrary, the p-OMe-substitution in **8** confers a 5-fold increase in potency. Compound **16**, bearing a furane ring, resulted in a loss of potency, probably due to a weaker interaction within the binding site.

According to our docking studies (Figure 4), the biaryl system fits into a region extending from the aromatic cage toward a receptor cavity which widens the agonist binding site, as documented by most of the AChBP cocrystal structures. Interestingly, the recently determined X-ray structure[26] (2Y58 PDB code) identifies a ligand-inducible subpocket of AChBP which partly overlaps with the region occupied by the biaryl system of series 2 compounds into our theoretical binding site. This receptor region is rich in lysine, asparagine, and tyrosine residues, which are prone to give hydrogen bonds to the ligand counterpart. In particular, K137 was predicted to H-bond to the

p-OMe substituent on the end aryl ring of compound **8**, while K139 was accessible for further interactions with the acceptor nitrogen on the pyrazole ring. Weaker EC$_{50}$ values of compounds **14** and **16** were likely to be due to a suboptimal distance of the hydrogen bond with K137.

Being that compound **8** was the most active, we decided to explore the effect of the -OMe substitution in the *ortho* and *meta* positions (compounds **9** and **10**), but we observed no benefit in terms of activity. In light of this result, we opted for substituents only in the *para* position for the other analogues. The effect of a methyl group on the pyrazole ring was also investigated (compound **11**) to evaluate the potential of branching our molecules, but the loss of activity was evident. This initial pool of molecules was also characterized in our selectivity panel of homologous receptor and in our ADME profiling assays. No agonist activity was observed on the α1, α3, and 5HT3 receptors for any of the compounds tested. Regarding the inhibitory activity, no problem of selectivity was observed for the homologous α1 and 5HT3 receptors, while all the compounds tested presented some activity against the ganglionic α3 receptor. With no exceptions, all the molecules showed excellent solubility, passive permeability, metabolic stability, and no cytochrome P450 inhibition. The p-OMe substituted compound **8** exhibited the best profile in terms of α7 activity, a selectivity ratio for the ganglionic α3 receptor (α3 IC$_{50}$/α7 EC$_{50}$) in line with the other analogues, and an optimal overall profile. For these reasons, it was considered the best tool for further SAR studies. The next

Table 3. ClogP, MPSA, Activity, Selectivity (EC$_{50}$ for Agonist Behavior, IC$_{50}$ for Antagonist Behavior), Solubility, Permeability (Perm Class), Metabolic Stability (% Remaining), and P450 Subtype Percent Inhibition at 3 µM, for a Representative Selection of Phenyl Pyrazole Derivatives in Which the Basic Center Is Explored

Compound	R	ClogP	MPSA (Å²)	Activity[a] EC$_{50}$ α7 (µM) ± SEM (n)	Selectivity[a] IC$_{50}$ (µM)			Sol[b] (µM)	Perm[c]	Met Stab[d] (%)	P450 inhibition[e] (%)		
					α1	α3	5HT3				3A4	2D6	2C9
8		3.9	70.3	0.43 ± 0.12 (3)	>30	3.25	>30	219	High	99	-5	4	-1
17		4.4	70.3	1.60 ± 0.24 (3)	NT	NT	NT	198	High	88	4	-4	-15
18		2.6	79.5	0.59 ± 0.11 (2)	>30	11.61	>30	176	High	100	19	2	-24
19		0.8	99.4	>30 (2)	NT	NT	NT	92	Low	100	-12	-5	-22
20		1.4	113.3	22.24 ± 8.76 (2)	NT	NT	NT	184	Low	100	-5	48	-15
21		4.4	70.3	1.05 ± 0.63 (2)	>30	>30	>30	133	High	100	3	21	-2
22		2.6	79.5	0.67 ± 0.23 (3)	>30	>30	>30	176	High	100	-14	-4	-18
23		2.0	82.3	5.41 ± 1.51 (2)	NT	NT	NT	153	Low	79	1	22	-1
24		2.1	99.4	>30 (2)	NT	NT	NT	117	Low	97	-2	-4	-28
25		1.90	90.6	0.18 ± 0.01 (28)	>30	>30	>30	170	Medium	95	-5	14	-8

[a]All functional activities were measured in either calcium flux or membrane potential assays using a fluorescence imaging plate reader. Compounds with E_{max} > 70% of nicotine were considered to be full agonists. The reported compounds gave values >90%. Only compounds with α7 activity lower than 1.5 µM were considered suitable for the selectivity evaluation. NT indicates not tested. [b]Solubilities were determined at pH 7.4 at pseudothermodynamic equilibrium. [c]Permeability was based on measuring the permeation rate of the test article through an artificial membrane. The PAMPA assay uses a mixture of porcine brain lipids in dodecane (2% w/v).[40] [d]Metabolic stability was determined as percentage remaining after incubation for 1 h with recombinant hCYP3A4. [e]Percent cytochrome inhibition values <15−20% were considered low. See Experimental Section for further details on all assays.

exploration phase concerned the modification of the region bearing the basic center.

Basicity is a determinant factor for the activity on the α7 receptor and explains why most α7 agonists contain a quinuclidine amine scaffold, bearing a strong basic center. Protonated nitrogen is required to make a key pharmacophoric interaction with the receptor binding site. The results observed and reported in Table 3 show that the basicity of the R substituent only appears to have a limited impact on the α7 activity. Compounds **8** and **18**, for example, are comparably active despite relatively different pK_a values (piperidine pK_a = 10.9, morpholine pK_a = 9.2).[27] We believe this observation to be valid as long as the pK_a is sufficient to have the basic nitrogen protonated at physiological pH.

At the same time, the α7 activity seems to be modestly affected by the ring size, as exemplified moving from piperidine to azepine (compounds **8** and **21**). These SAR studies showed strong evidence of the detrimental effect on activity, derived from an extra hydrogen bond donor, which also confers the molecules higher MPSA and lower ClogP values. The additional NH moiety leads to an increase in the hydrophilicity of the R substituents which was not tolerated in this position. This is proven by the loss of activity in compounds **19**, **20**, **23**, and **24**, with the exclusion of the steric hindrance effect, as demonstrated by the good activity of compound **25**.

In the putative binding mode of compound **25** into the theoretical model of α7 receptor (Figure 5), the acetyl-diazepane moiety fits the cavity hosting the nicotine structure in the AChBP cocrystal structures. This cavity was in part delimited by the W143 and Y192 residues of the aromatic cage
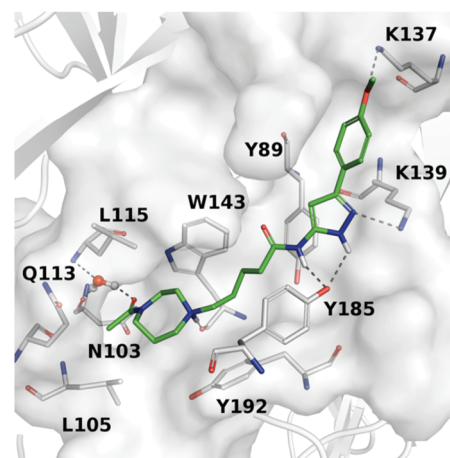

Figure 5. Predicted binding mode of compound **25**. Important active site residues are labeled. Potential hydrogen bonds are shown as dotted lines.

and the residues L105, Q113, and L115. The pocket was large enough to accommodate substituted 6−7 membered rings and has mainly a lipophilic nature, which may account for the drop in activity of more polar compounds such as **19**, **20**, **23**, and **24**. In the docked poses of compound **25** into the α7 homology model, the acetyl−diazepane system mimics the pyrrolidine−pyridine system of nicotine: the protonated nitrogen was ideally positioned to target W143, whereas the carbonyl group was bound to L115 and N103 through a bridging water molecule, such as the pyridine nitrogen of nicotine and many other α7 agonists. The X-ray structures of some recently published diazepane−pyridine α7 agonists bound to AChBP nicely agree with the predicted interaction network established by the acetyl−diazepane system of our molecules (3U8M, 3U8K, 3U8N, 3U8J, 3U8L PDB codes). The amide-pyrazole system and the terminal *p*-methoxy substituent of compound **25** maintain the previously described contacts with the receptor, with the former being involved in an optimal interaction with Y185 and K139, and the latter in a hydrogen bond to K137. In terms of selectivity, no issues were highlighted in Table 3 for the α1 and 5HT3 receptors. Some cross-reactivity on the ganglionic α3 receptor was present for compounds **8** and **18**, while no activity was observed on all the other analogues present in Table 3. This better profile was likely due to the higher steric hindrance of compounds **21**, **22**, and **25** compared to **8** and **18** not being tolerated by the α3 receptor.

While all the analogues presented an optimal profile in terms of solubility, metabolic stability, and cytochrome P450 inhibition, passive permeability for this series of compounds was sometimes nonoptimal. The general trend was that compounds with lower permeability were those with lower ClogP and higher MPSA.
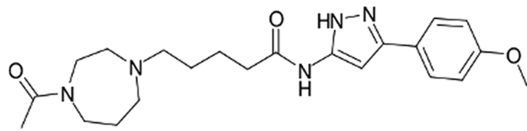
On the basis of the collective data, compound **25** was selected to be progressed for further studies. Although its permeability fell into the medium class, this was counterbalanced by the excellent spectrum of activity, selectivity, and the rest of the profiling data.

The physicochemical properties, additional pharmacology, ADME properties, and pharmacokinetic profile for compound **25** are summarized in Table 4, where MW, ClogP, ClogD, and MPSA were in line for potential brain penetration. The affinity of compound **25** for the receptor was confirmed in a binding assay using the rat receptor (0.66 μM). The potency was further demonstrated in electrophysiological studies in both rat and human receptor expressing cell lines (4.4 and 3.0 μM, respectively, full agonist functional responses). The hERG inhibition was considered acceptable to forecast low potential for cardiotoxicity issues. In addition, compound **25** did not show any cross-activity in a broad panel of 70 receptors (% inhibition <50 at 10 μM). In terms of ADME properties, the *in vitro* intrinsic clearance in rat was optimal (13.0 μL/min/mg) and the plasma stability was acceptable (55% after 3 h incubation) while the *in vitro* permeability in the MDCK cell line, although nonoptimal, was considered not limiting for further progression of the molecule ($P_{app A \rightarrow B}$ 1.6 × 10^{-6} cm/s, efflux ratio 4.6). Compound **25** was progressed to a PK study and showed an overall moderate exposure, in particular low bioavailability (12%) and moderate brain to plasma partitioning and brain levels (0.38 B/P ratio and 3.7 ng/g, respectively).

In light of the brain levels observed, we decided to evaluate compound **25** in behavioral animal tests.

The estimation of the brain concentration of other α7 agonists (for example PHA-543,613)[28] to achieve efficacy in

Table 4. Selected Physicochemical Properties, Additional Pharmacology, ADME, and Rat Pharmacokinetic Data for 25

physicochemical properties	MW	413.51 Da
	cLogP	1.90
	cLogD at pH 7.4	1.69
	MPSA	90.6 Å^2
additional pharmacology	α7 K_i (rat)^a	0.66 μM
	α7 e-phys^b EC$_{50}$ (rat, hu)	4.4 μM, 3.0 μM
	α7 e-phys^b E$_{max}$ (rat, hu)	99%, 89%
	hERG^c IC$_{50}$	24.2 μM
ADME	plasma stability 3 h^d	55%
	Cl$_{int}$ (rat)^e	13.0 μL/min/mg
	MDCK AB^f	1.6 × 10^{-6} cm/s
	MDCK BA/AB^g	4.6
PK rat (20 mpk, po)	C$_{max}$^{h}	0.18 μM
	T$_{max}$^{h}	0.83 h
	AUC$_{0-inf}$^{h}	1.37 μM·h
	F^i	12%
BBB rat (10 mpk, po)	B/P^j	0.38
	C$_{max}$^{j}	3.7 ng/g

^{a}Binding assay for human α7 nAChR expressed in GH4C1 cells using [^{3}H]-epibatidine as the radioligand. ^{b}Whole cell patch clamp recordings were performed on GH4C1 cells expressing rat α7 receptors or CHO cells expressing the human α7 receptor with Ric-3. Each cell was exposed to at least one concentration of acetylcholine and a full range of concentrations of **25**. ^{c}hERG response was obtained from CHO cells stably expressing the channel using an IonWorks system. ^{d}Plasma stability was determined as percentage remaining after incubation for 3 h with fresh rat plasma. ^{e}*In vitro* intrinsic clearance from rat liver microsomal stability assay. ^{f}MS-based quantification of apical → basolateral transfer rate of a test compound at 10 μM across contiguous monolayers of MDCK cells. ^{g}Ratio of (basolateral → apical) to (apical → basolateral) transfer rate of a test compound at 10 μM across contiguous monolayers of MDCK (Madin−Darby canine kidney) cells. ^{h}Pharmacokinetic parameters were determined following a single 20 mg/kg po dose in male Long Evans rats. ^{i}Oral bioavailability (F) was determined in a separate experiment as the ratio of AUC$_{0-inf}$ normalized for the dose, obtained following single 10 mg/kg iv doses in male Long Evans rats. ^{j}The brain to plasma (B/P) ratio was determined as the ratio of AUC$_{0-inf}$ following a single 10 mg/kg po dose in male Long Evans rats.

vivo, during behavioral tests, is not sufficient to activate α7 nAChRs *in vitro*. This observation encouraged us to advance our compound to *in vivo* efficacy evaluation, even in the presence of moderate brain exposure. Compound **25** displayed efficacy in assays of cognitive function in the rat model, namely in a form of episodic memory measured in the novel object recognition test (NOR, Figure 6A). In perceptual processing, **25** showed the ability to attenuate pharmacologically induced deficits via the glutamatergic system in a prepulse inhibition model (PPI, Figure 7), a classic paradigm for evaluating potential treatment for schizophrenia. In agreement with our findings, very recently[29] the positive outcome of *in vivo* experiments even at *in vitro* subpharmacological doses has been

Figure 7. Ability of compound **25** to normalize an MK-801 induced disruption of prepulse inhibition (PPI) of the acoustic startle response in rats ($n = 7−8$ treatment group). Blue column, vehicle no. MK-801; red columns, vehicle or compound **25** at several doses administered orally. Statistical analysis, ANOVA and Fisher's LDS test; * $P < 0.05$ vs MK-801 plus vehicle.
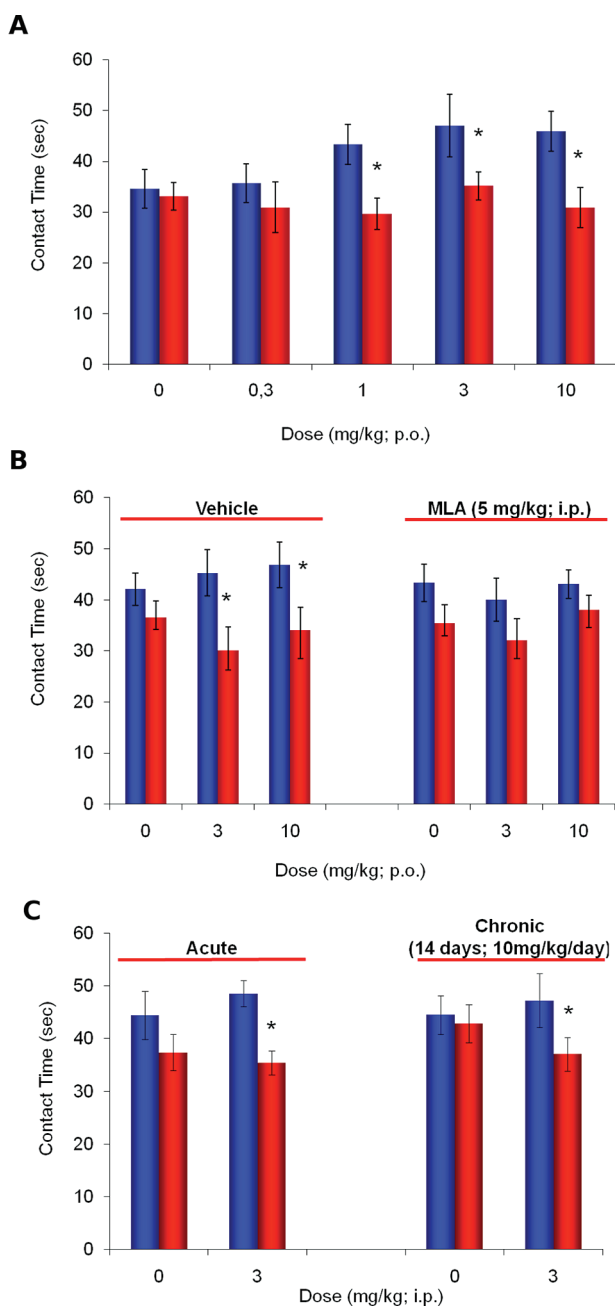

Figure 6. Induced memory enhancement of **25** in a novel object recognition test (NOR) using spontaneous decay of memory (48 h time-interval) as the amnesic factor in rats ($n = 10−12$ treatment group). Blue columns, exploration time of new object; red columns, exploration time of familiar object. (A) Effects of several doses of **25** administered orally 1 hour before T1 exploration. (B) Reversion of memory enhancement induced by **25** using pretreatment (5 min before the orally administration of **25**) with MLA. (C) Lack of tolerance to compound **25** in NOR: the effect is maintained after 14 days of intraperitoneal administration of **25** and is analogous to the acute administration. Statistical analysis: ANOVA and Fisher's LDS test: * $P < 0.05$ vs time in exploring a familiar object.

interpreted as the coagonist activity of EVP-6124 with acetylcholine on α7 nAChRs.

Treatment with **25** induced a memory enhancement in the NOR at several doses when administered orally, using a 48 h delay time as the amnesic factor, with a minimum efficaci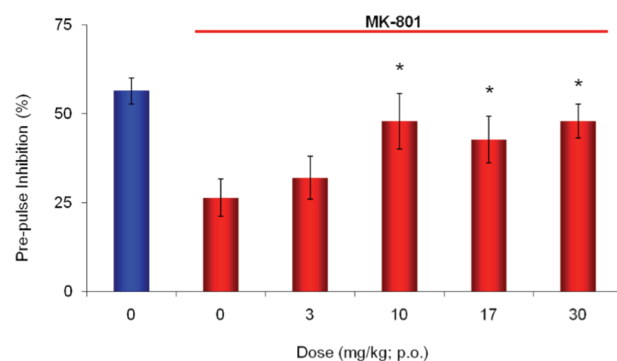ous dose of 1 mg/kg (Figure 6A). Importantly, the induced memory enhancement in the NOR experiment was blocked by the pretreatment with the α7 antagonist methyllycaconitine (MLA), demonstrating the direct involvement of the α7 nAChR (Figure 6B). In addition, to evaluate any tolerance to this behavioral effect, **25** was administered once daily for 14 days before the NOR test. It demonstrated retention of acute memory enhancing activity in chronically exposed animals comparable to that of animals just given an acute treatment, showing no loss of the *in vivo* signal with chronic daily dosing and potentially no tolerance to the compound (Figure 6C).

Moreover, compound **25** administered orally reversed (+)-5-methyl-10,11-dihydro-5H-dibenzo[a,d]cyclohepten-5,10-imine (dizocilpine, MK-801)-induced deficits in the PPI in rat with a minimum efficacious dose of 10 mg/kg (Figure 7).
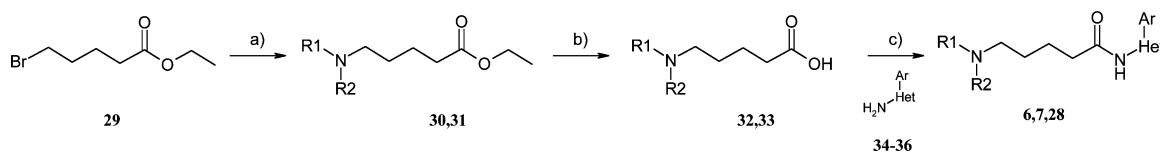
The excellent *in vivo* pharmacological profile displayed by compound **25**, despite the nonoptimal properties in the ADME and PK areas, prompted us in the continuation of the α7 program. To further explore the chemical space around compound **25**, we performed pinpoint modifications aimed at improving passive permeability and plasma stability. We explored the introduction of a methyl group both on the pyrazole ring and in the position α to the carbonyl of the amide group (Table 5, compounds **26** and **27**, respectively). We also explored the replacement of the pyrazole ring with the regioisomer imidazole ring (**28**). The idea behind the introduction of an extra methyl group was to improve passive permeability by increasing ClogP, and plasma stability by hindering the amide bond (which is known to be susceptible to hydrolysis by plasma esterases). The replacing of the pyrazole by the imidazole ring was aimed at introducing a five membered heterocycle with a hydrogen bond donor function and a different heteroatoms arrangement (with respect to pyrazole) to potentially improve the plasma stability by altering the electronic character of the amide bond. The biological results showed that introduction of the methyl group on the pyrazole ring, as noted before, was detrimental for activity as well as the imidazole/pyrazole exchange. Interestingly, the extra methyl group in the position α to the carbonyl of the amide maintained a good level of potency, improved the passive permeability, and ameliorated the plasma stability. This modification seemed to confer a better overall profile to compound **27** compared to compound **25**, paving the way for further exploration both of our chemical series and of compound **27**.

Table 5. ClogP, MPSA, Activity, Selectivity (EC_{50} for Agonist Behavior, IC_{50} for Antagonist Behavior), Solubility, Permeability (Perm Class), Metabolic Stability (% Remaining), P450 Subtype Percent Inhibition at 3 μM, and Plasma Stability (% Remaining, 3 h), for a Representative Selection of Phenyl Pyrazole Derivatives in Which the Cental Linker Region Is Explored

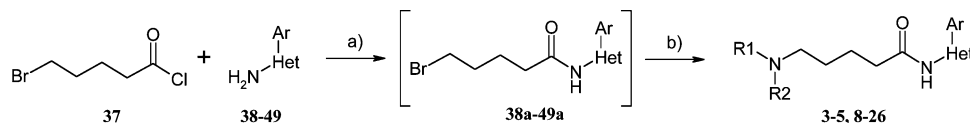| Compound	Structure	ClogP	MPSA (Å^2)	Activity[a] EC_{50} α7 (μM) ± SEM (n)	Selectivity[a] IC_{50} (μM)			Sol[b] (μM)	Perm[c]	Met Stab[d] (%)	P450 inhibition[e] (%)			Plasma Stability[f] 3h (%)
					α1	α3	5HT3				3A4	2D6	2C9	
25		1.90	90.6	0.18 ± 0.01 (28)	>30	>30	>30	170	Medium	95	-5	14	-8	55
26		2.17	90.56	6.83 ± 2.75 (2)	NT	NT	NT	151	Medium	100	1	-9	-13	NT
27		2.21	90.55	0.36 ± 0.02 (2)	>30	>30	>30	128	High	100	0	5	2	>99
28		1.74	90.56	3.47 ± 1.46 (2)	NT	NT	NT	193	High	100	5	15	12	NT

[a]All functional activities were measured in either calcium flux or membrane potential assays using a fluorescence imaging plate reader. Compounds with E_{max} > 70% of nicotine were considered to be full agonists. The reported compounds gave values >90%. Only compounds with α7 activity lower than 1.5 μM were considered suitable for the selectivity evaluation. NT indicates not tested. [b]Solubilities were determined at pH 7.4 at pseudothermodynamic equilibrium. [c]Permeability was based on measuring the permeation rate of the test article through an artificial membrane. The PAMPA assay uses a mixture of porcine brain lipids in dodecane (2% w/v).[40] [d]Metabolic stability was determined as the percentage remaining after incubation for 1 h with recombinant hCYP3A4. [e]Percent cytochrome inhibition values <15−20% were considered low. [f]Plasma stability was determined as the percentage remaining after incubation for 3 h with fresh rat plasma. See the Experimental Section for further details on all assays.

Scheme 1. Synthesis of 5-Aminopentanoic Acid Amide via Route A[a]

[a](a) R1R2NH, toluene, reflux; (b) NaOH, water, reflux; (c) CDI, 1,2-dichloroethane, 50 °C.

Scheme 2. Synthesis of 5-Aminopentanoic Acid Amide via Route B[a]

[a](a) DIPEA, DMA, −10 °C; (b) Route B1: R1R2NH, NaI, DMA, 50 °C or Route B2: R1R2NH, NaI, DMF, 60 °C.

■ CHEMISTRY

The compounds investigated, with the exception of **27**, were synthesized using one of the two general routes reported in Schemes 1 and 2 (routes A and B, respectively).

Even though route A could be preferred for the chemical exploration of the biaryl system and route B for the basic moiety, the two synthetic strategies were equally efficient in terms of yields and synthetic difficulty. Therefore, they were used indifferently by us. In route A (Scheme 1), commercially available ethyl 5-bromopentanoate **29** was reacted with a secondary amine through a nucleophilic substitution reaction to give the desired ethyl 5-aminopentanoate derivatives **30** and **31**; the esters were then hydrolyzed with NaOH to give the corresponding 5-aminopentanoic acids **32** and **33**. Subsequently, the acids **32** and **33** were coupled to 3-amino-5-aryl heterocycle (**34–36**) (Chart 1) with N,N'-carbonyldiimidazole in dichloroethane to afford the targeted products aminopentanoic acid amide (**6**, **7**, and **28**).

In route B (Scheme 2), 5-bromovaleroyl chloride (**37**) was reacted with 3-amino-5-aryl/heteroaryl heterocycles (**38–49**)

Chart 1. 3-Amino-5-aryl Heterocycle Used in Route A

Compound	Structure
34	
35	
36	

(Chart 2) in dimethylacetamide to give the corresponding 5-bromopentanoyl amide (**38a–49a**).

In the case of 3-amino-5-aryl/heteroaryl pyrazoles (**39–49**), the acylation on the endocyclic nitrogen of the pyrazole ring to give products **39b–49b** was also detected together with an intramolecular cyclization of **39a–49a** to give products **39c–49c** (Scheme 3). After a rapid screening of solvents, dimethylacetamide was selected as the best medium to minimize these side reactions (in dimethylacetamide usually less than 10% of acylation on the endocyclic nitrogen was observed and only traces of the intramolecular cyclization).

Chart 2. 3-Amino-5-aryl/Heteroaryl Heterocycles Used in Route B

Compound	Structure
38	
39	
40	
41	
42	
43	
44	
45	
46	
47	
48	
49	

The 5-bromopentanoyl amide (**38a−49a**) obtained was either reacted *in situ* (route B1) with the addition of a secondary amine and NaI or isolated by precipitation with water (route B2) and reacted with a secondary amine and NaI in dimethylformamide to afford the final 5-aminopentanoic acid amide (**3−5, 8−26**).

Compound **27** was synthesized according to route C: 2-methyl-malonic acid dimethyl ester **50** was treated with NaH, in tetrahydrofurane and reacted with 1,4-dibromopropane **51**, through a nucleophilic substitution reaction (Scheme 4). The disubstituted dimethyl malonate **52**, thus obtained, was hydrolyzed and monodecarboxylated by treatment with HBr to obtain 5-bromo-2-methylpentanoic acid (**53**). The acid **53** was activated with oxalyl chloride and coupled to 5-amino-3-(4-methoxyphenyl)pyrazole-1-carboxylic acid *tert*-butyl ester (**54**) in dichloromethane to afford 5-bromopentanoyl amide **55**. This reaction required the use of the Boc protected pyrazole **54** in order to avoid acylation on the endocyclic nitrogen of the pyrazole. Compound **55** was then subjected to a nucleophilic substitution reaction with acetyldiazepine in dichloromethane

to afford 5-aminopentanoic acid amide Boc protected **56**, which was treated with HCl in dioxane to remove Boc protection and afford the desired 5-aminopentanoic acid amide **27**.

3-Amino-5-aryl/heteroaryl heterocycles, **34−36, 38−43**, and **46** were found to be commercially available, while 3-amino-5-aryl/heteroaryl pyrazoles **44, 45**, and **47−49** were synthesized according to literature procedures.[30−32]

■ CONCLUSIONS

Most of the α7 agonists reported to date belong to the quinuclidine amine family.[19] Our research group concentrated its efforts in designing different scaffolds in order to add novelty to our compounds and preempt potential risks associated with this structure. Interestingly, recent literature reported the failure in clinical phase trials of quinuclidine containing α7 agonists due to toxicological reasons, corroborating our initial strategic choice. For example, PHA568,487 was discontinued for cardiovascular findings of nonsustained ventricular tachycardia in human; this type of toxicity is probably to be ascribed to this structural class.[33]
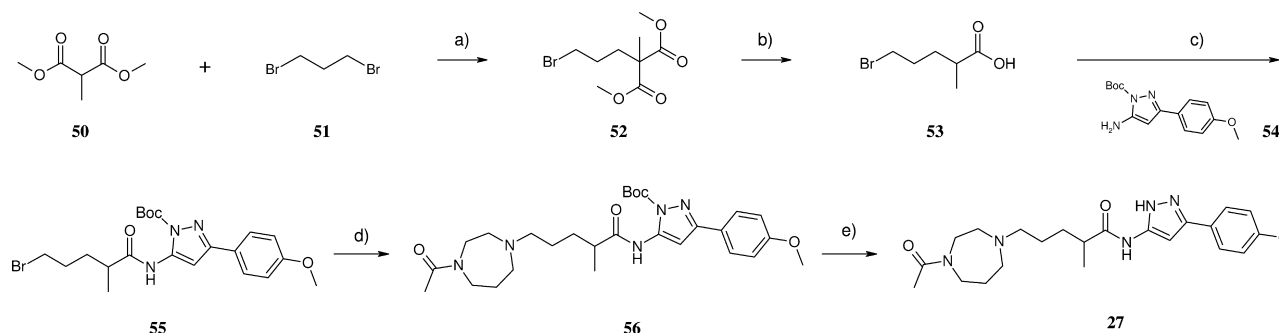
Our continuous efforts in the α7 agonist area led us to the identification of a novel chemical series which, in line with our focus, does not belong to the quinuclidine amine family. This series emerged from a chemical exploration of our previously reported structures and improves both selectivity and ADME profiling. One of these molecules (compound **25**, SEN15924, WAY-361789) was characterized in behavioral studies in light of the good potency, selectivity, ADME profile, and acceptable PK and was found to improve cognitive function in NOR and to reverse a pharmacological disruption in PPI. Recent structural modification of compound **25** confirmed the possibility of improving its overall profile and potentially offers an attractive candidate (for example, compound **27**) worthy of further investigation.

■ EXPERIMENTAL SECTION

1. Chemistry. General Methods. Unless otherwise specified, all nuclear magnetic resonance spectra were recorded using a Varian Mercury Plus 400 MHz spectrometer equipped with a PFG ATB broadband probe. UPLC-MS analyses were run using a Acquity Waters UPLC equipped with a Waters SQD (ES ionization) and Waters Acquity PDA detector, using a column BEH C18 1.7 μm, 2.1 mm × 50 mm. Gradients were run using 0.1% NH_4HCO_3 water/acetonitrile 95/5 and acetonitrile with a gradient 95/5 to 15/85, flow: 0.8 mL/min over 3 min or 0.05% formic acid water/acetonitrile 95/5 and acetonitrile with a gradient 95/5 to 100, flow: 0.8 mL/min as stated in the examples. Retention times were expressed in minutes. Temperature: 40 °C. UV detection at 215 nm and 254. ESI+ detection in the 80−1000 m/z range. Preparative HPLC was run using a Waters 2767 system with a binary gradient module Waters 2525 pump and coupled to a Waters Micromass ZQ (ES) or Waters 2487 DAD, using

Scheme 3. Acylation of Aminopyrazoles (39−49) and Side Products[a]

spontaneous cyclization
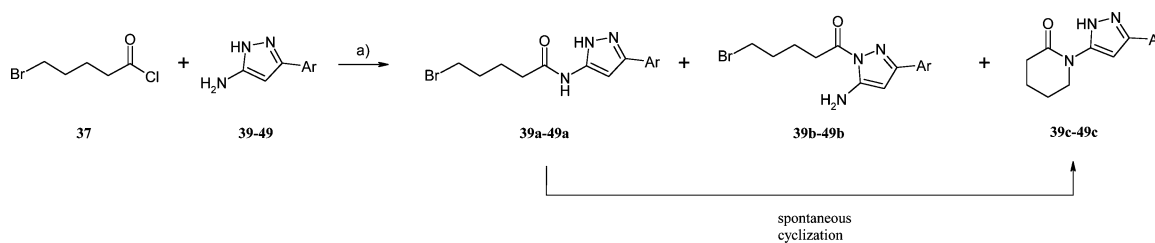
[a](a) DIPEA, DMA, −10 °C.

Scheme 4. Synthesis of Compound 27 via Route C[a]

[a](a) NaH, THF, 0 °C; (b) HBr 48%, 110 °C; (c) (COCl)$_2$, NEt$_3$, DCM, RT; (d) acetyldiazepine, NEt$_3$, DCM, 50 °C; (e) HCl, dioxane, RT.

a X-Bridge C18 5 μm, 19 mm × 150 mm, using a 0.1% formic acid/water and 0.1% formic acid/methanol flow: 17 mL/min. The purity of compounds submitted for screening was >95% as determined by integrating at 215 nm the peak area of the LC chromatograms. To further support the purity statement, all compounds were also analyzed at a different wavelengths (254 nm), and total ion current (TIC) chromatogram and NMR spectra were used to further substantiate results. HRMS data were obtained through an LTQ-Orbitrap mass spectrometer via direct infusion of a 1 μM sample in acetonitrile 30%/water 69.9%/formic acid 0.1% (flow: 7 μL/min). The LTQ-Orbitrap instrument was calibrated prior to analysis with the manufacturer's positive ion Calibration Solution in the mass range 100−2000 m/z. Each determination was the combination of five successive scans acquired at 100.000 fwhm resolution. Elemental composition calculations and isotopic pattern simulations were executed using the specific tool included in the QualBrowser module of Xcalibur (Thermofisher Scientific, release 2.0.7) software, using a tolerance of 5 ppm. All column chromatography was performed following small modifications of the original method of Still.[34] All TLC analyses were performed on silica gel (Merck 60 F254) and spots revealed by UV visualization at 254 nm and KMnO$_4$ or ninhydrin stain.

2. Synthesis. General Procedure for 5-Aminopentanoic Acid. To a solution of amine (65 mmol) in toluene (15 mL) was added ethyl 5-bromopentanoate (26 mmol), and the reaction mixture was refluxed for 10 h. The mixture was allowed to cool to room temperature, and any solid present was filtered off and washed with ether. The filtrate was concentrated under reduced pressure to give ethyl 5-aminopentanoate, which was used in the next step without further purification. To a suspension of crude ethyl 5-aminopentanoate from the previous step (about 25 mmol) in 15 mL of water was added NaOH (1.4 g, 25 mmol), and the mixture was heated at reflux for 16 h. The reaction was then allowed to cool down to room temperature, and the solution was acidified at 0 °C with HCl 6 N and concentrated under reduced pressure. The residue was treated with EtOH, and the precipitated sodium chloride was filtered off. Evaporation of the solvent under reduced pressure afforded the 5-aminopentanoic acid as a white solid.

5-Piperidin-1-ylpentanoic Acid Hydrochloride (32). Following the general procedure for 5-aminopentanoic acid and starting from the commercially available ethyl 5-bromopentanoate (29, 2.0 g, 9.6 mmol), 1.9 g of title compound as hydrochloride was obtained (90% yield). ^{1}H NMR (400 MHz, DMSO-d_6): δ 1.39−1.58 (m, 4H), 1.61−1.80 (m, 6H), 2.19−2.27 (m, 2H), 2.69−3.50 (m, 7H), 11.40 (br s, 1H). Mass (ES) m/z: 186 (M + 1).

5-(4-Acetyl[1,4]diazepan-1-yl)pentanoic Acid (33). Following the general procedure for 5-aminopentanoic acid and starting from the commercially available ethyl 5-bromopentanoate (29, 2.0 g, 9.6 mmol), 2.2 g of title compound was obtained by acidification to the isoelectric point (83% yield). ^{1}H NMR (400 MHz, CDCl$_3$): δ 1.37−1.57 (m, 4H), 1.76−1.90 (m, 2H), 2.09 (s, 3H), 2.10−2.16 (m, 2H), 2.36−2.45 (m, 2H), 2.53−2.66 (m, 4H), 3.44−3.63 (m, 4H), 11.38 (br s, 1H). Mass (ES) m/z: 241 (M − 1).

General Procedure for 5-Aminopentanoic Acid Amide. Route A. To a suspension of 5-aminopentanoic acid (7.93 mmol) in 1,2-dichloroethane (20 mL) was added N,N′-carbonyldiimidazole (1.2 g, 7.4 mmol), and the mixture was stirred at room temperature for 2 h (when the activation of the amino acid was complete, dissolution of the suspension was generally observed). The 3-amino-5-aryl/heteroaryl heterocycle (5.29 mmol) was then added, and the reaction was stirred for further 10 h. Upon reaction completion (as monitored by LC-MS) if the formation of two isomers was observed, the mixture was heated at 50 °C until the conversion of the less stable isomer to the title compound was observed (as monitored by LC-MS). The solvent was washed with sat. Na$_2$CO$_3$ solution, extracted, and removed under reduced pressure. The crude products were either recrystallized from CH$_3$CN or purified by SiO$_2$ column chromatography or by preparative HPLC.

5-Piperidin-1-ylpentanoic Acid [5-(4-Chlorophenyl)[1,3,4]-thiadiazol-2-yl] Amide (6). Following the general procedure for 5-aminopentanoic acid amide A and starting from commercially available 5-(4-chlorophenyl)[1,3,4]thiadiazol-2-ylamine (34, 96.0 mg, 0.45 mmol), 42.0 mg of title compound as formate salt was obtained by preparative HPLC (25% yield). ^{1}H NMR (400 MHz, DMSO-d_6): δ 1.30−1.39 (m, 2H), 1.38−1.50 (m, 5H), 1.52−1.65 (m, 2H), 2.22−2.36 (m, 5H), 2.48−2.53 (m, 4H), 7.54−7.60 (m, 2H), 7.90−7.97 (m, 2H), 8.17 (s, 1H), 10.30 (s, 1H). ^{13}C NMR (DMSO-d_6): δ 172.37, 161.07, 159.42, 135.71, 130.06, 129.82, 129.20, 112.24, 58.64, 54.59, 35.44, 26.28, 26.18, 24.71, 23.27. Mass (ES) m/z: 379 (M + 1). UPLC (basic method); R$_t$ = 1.29 min; area 100%. HRMS: calcd for C$_{18}$H$_{23}$ClN$_4$OS + H$^+$, 379.13539; found (ESI, [M + H]$^+$ obsd), 379.13525.

5-Piperidin-1-ylpentanoic Acid [3-(4-Chlorophenyl)isoxazol-5-yl] Amide (7). Following the general procedure for 5-aminopentanoic acid amide A and starting from commercially available 3-(4-chlorophenyl)-isoxazol-5-ylamine (35, 88.0 mg, 0.45 mmol), 28.0 mg of title compound as formate salt was obtained as a solid by preparative HPLC (18% yield). ^{1}H NMR (400 MHz, CD$_3$OD): δ 1.5−1.90 (m, 10H), 2.50−2.57 (m, 2H), 3.05−3.12 (m, 2H), 3.03−3.28 (m, 4H), 6.70 (s, 1H), 7.47−7.51 (m, 2H), 7.76−7.82 (m, 2H), 8.49 (s, 1H). ^{13}C NMR (CD$_3$OD): δ 170.36, 169.01, 162.55, 162.37, 136.04, 130.70, 129.07, 128.01, 86.09, 57.17, 53.38, 34.91, 23.89, 23.63, 22.13, 22.08. Mass (ES) m/z: 362 (M + 1). UPLC (basic method); R$_t$ = 1.40 min; area 100%. HRMS: calcd for C$_{19}$H$_{24}$ClN$_3$O$_2$ + H$^+$, 362.16298; found (ESI, [M + H]$^+$ obsd), 362.16291.

5-(4-Acetyl[1,4]diazepan-1-yl)pentanoic Acid [5-(4-Methoxy-phenyl)-1H-imidazol-2-yl] Amide (28). Following the general procedure for 5-aminopentanoic acid amide A and starting from commercially available 5-(4-methoxyphenyl)-1H-imidazol-2-ylamine (36, 260.0 mg, 1.37 mmol), 77 mg of title compound (14%, yield) was obtained as a solid by SiO$_2$ column chromatography (ACN/MeOH NH$_3$ 2 M 90:10). ^{1}H NMR (400 MHz, CD$_3$OD): δ 1.53−1.63 (m, 2H), 1.64−1.76 (m, 2H), 1.77−1.97 (m, 2H), 2.09 (s, 3H), 2.45 (t, J = 7.3 Hz, 2H), 2.49−2.59 (m, 2H), 2.63−2.77 (m, 4H), 3.52−3.69 (m, 4H), 3.79 (s, 3H), 6.91 (d, J = 8.7 Hz, 2H), 7.04 (s, 1H), 7.57 (d, J = 8.6 Hz, 2H). ^{13}C NMR (CD$_3$OD): δ 172.98, 171.87, 158.98,

141.67, 135.71, 134.74, 125.81, 113.90, 109.81, 57.15, 55.55, 54.57, 54.14, 44.29, 44.08, 35.44, 27.31, 26.13, 23.14, 20.45. Mass (ES) m/z: 414 (M + 1). UPLC (basic method); R_t = 0.92 min; area 100%. HRMS: calcd for $C_{22}H_{31}N_5O_3$ + H$^+$, 414.24997; found (ESI, [M + H]$^+$ obsd), 414.24984.

General Procedure for 5-Aminopentanoic Acid Amide. Route B1, Two Steps Synthesis. A solution of 5-bromovaleroyl chloride (15.7 mmol, 1 equiv) in dry DMA (35 mL) was cooled to −10 °C (ice/water bath) under N$_2$; a solution of 3-amino-5-aryl/heteroaryl heterocycle (15.7 mmol, 1 equiv) and diisopropylethylamine (15.7 mmol, 1 equiv) in dry DMA (15 mL) was added over 30'. After 2 h at −10 °C, completion of the reaction, as monitored by LC-MS, was generally observed (in the case of pyrazole, acylation on the pyrazole ring was also detected). The reaction was then quenched by addition of H$_2$O (ca. 50 mL); the thick white precipitate formed upon addition of water was recovered by filtration. Washing with Et$_2$O (3 × 10 mL) usually efficiently removed the byproduct of acylation on the pyrazole ring in the case of pyrazole.

5-Bromopentanoic acid amide (0.6 mmol, 1 equiv) was dissolved in DMF (4 mL), and sodium iodide (0.6 mmol, 1.0 equiv) was added followed by the secondary amine (1.5 mmol, 2.5 equiv) and diisopropylethylamine (0.6 mmol, 1 equiv). The reaction was then stirred under N$_2$ at +50 °C for 18 h. Upon reaction completion (as monitored by LC-MS), the solvent was removed at reduced pressure, and the resulting oily residue was dissolved in DCM (20 mL), washed with sat. Na$_2$CO$_3$ (2 × 20 mL) and sat. NaCl (2 × 20 mL); the organic layer was dried over Na$_2$SO$_4$ and the solvent removed under reduced pressure. The title compounds were purified by either SiO$_2$ column or preparative HPLC (standard acidic conditions).

5-Piperidin-1-ylpentanoic Acid [5-(4-Chlorophenyl)-2-methyl-2H-pyrazol-3-yl] Amide (4). Following the general procedure for 5-aminopentanoic acid amide B1 and starting from commercially available 5-(4-chlorophenyl)-2-methyl-2H-pyrazol-3-ylamine (**40**, 132 mg, 0.64 mmol), 70.0 mg of title compound as the formate salt was obtained by preparative HPLC (26%, yield). ^{1}H NMR (400 MHz, DMSO-d_6): δ 1.35−1.47 (m, 2H), 1.49−1.66 (m, 8H), 2.37−2.42 (m, 2H), 2.54−2.69 (m, 6H), 3.68 (s, 3H), 6.64 (s, 1H), 7.41 (d, J = 8.7 Hz, 2H), 7.74 (d, J = 8.7 Hz, 2H), 8.14 (s, 1H), 9.97 (s, 1H); ^{13}C NMR (DMSO-d_6): δ 171.59, 164.75, 147.62, 138.61, 132.96, 132.48, 129.30, 127.09, 96.75, 57.41, 53.55, 36.54, 35.52, 24.93, 24.59, 23.33, 23.15. Mass (ES) m/z: 375 (M + 1). UPLC (basic method); R_t = 1.22 min; area 100%. HRMS: calcd for $C_{20}H_{27}ClN_4O$ + H$^+$, 375.19462; found (ESI, [M + H]$^+$ obsd), 375.19458.

5-Piperidin-1-ylpentanoic Acid [5-(4-Methoxyphenyl)-2H-pyrazol-3-yl] Amide (8). Following the general procedure for 5-aminopentanoic acid amide B1 and starting from commercially available 5-(4-methoxyphenyl)-2H-pyrazol-3-ylamine (**39**, 95 mg, 0.50 mmol), 51 mg of title compound was obtained by SiO$_2$ column chromatography (DCM/MeOH 90:10) (28% yield). ^{1}H NMR (400 MHz, CD$_3$OD): δ 1.46−2.01 (m, 10H), 2.35−2.49 (m, 2H), 2.77−3.58 (m, 6H), 3.78 (s, 3H), 6.72 (bs, 1H), 6.91 (d, J = 8.4 Hz, 2H), 7.51 (d, J = 8.5 Hz, 2H); ^{13}C NMR (CD$_3$OD): δ 171.93, 160.24, 147.02, 144.52, 126.68, 122.67, 114.25, 93.28, 56.70, 54.69, 53.15, 34.98, 23.40, 23.12, 22.32, 21.52. Mass (ES) m/z: 357 (M + 1). UPLC (acid method); R_t = 0.79 min; area 100%. HRMS: calcd for $C_{20}H_{28}N_4O_2$ + H$^+$, 357.22850; found (ESI, [M + H]$^+$ obsd), 357.22830.

Synthesis of 5-(4-Methylpiperidin-1-yl)pentanoic Acid [5-(4-Methoxyphenyl)-2H-pyrazol-3-yl] Amide (17). Following the general procedure for 5-aminopentanoic acid amide B1 and starting from commercially available 5-(4-methoxyphenyl)-2H-pyrazol-3-ylamine (**39**, 57 mg, 0.30 mmol), 57 mg of title compound was obtained as the formate salt by purification with preparative HPLC (45% yield). ^{1}H NMR (400 MHz, DMSO-d_6): δ 0.85 (d, J = 6.5 Hz, 3H), 0.97−1.20 (m, 3H), 1.32 (m, 2H), 1.46−1.39 (m, 2H), 1.51 (dt, J = 14.8, 8.5 Hz, 3H), 1.96 (dd, J = 19.8, 9.1 Hz, 2H), 2.27 (t, J = 7.2 Hz, 2H), 2.34 (dd, J = 17.9, 10.7 Hz, 2H), 2.97−2.81 (m, 2H), 3.75 (s, 3H), 6.72 (s, 1H), 7.11−6.81 (m, 2H), 7.71−7.43 (m, 2H), 8.19 (s, 1H), 10.33 (s, 1H). ^{13}C NMR (CD$_3$OD): δ 171.88, 169.02, 160.23, 146.92, 144.55, 126.66, 122.73, 114.23, 93.18, 56.32, 54.63, 52.49, 34.98, 31.07, 28.61,

23.51, 22.40, 20.06. Mass (ES) m/z: 371 (M + 1). UPLC (acid method); R_t = 0.88 min; area 100%. HRMS: calcd for $C_{21}H_{30}N_4O_2$ + H$^+$, 371.24415; found (ESI, [M + H]$^+$ obsd), 371.24383.

Synthesis of 5-(3-Oxopiperazin-1-yl)pentanoic Acid [5-(4-Methoxyphenyl)-2H-pyrazol-3-yl] Amide (19). Following the general procedure for 5-aminopentanoic acid amide B1 and starting from commercially available 5-(4-methoxyphenyl)-2H-pyrazol-3-ylamine (**39**, 57 mg, 0.30 mmol), 28 mg of the title compound was obtained by purification with preparative HPLC (22% yield). ^{1}H NMR (400 MHz, DMSO-d_6): δ 1.21−1.26 (m, 1H), 1.33−1.66 (m, 3H), 2.26−2.32 (m, 2H), 2.47−2.53 (m, 2H), 2.78−3.02 (m, 2H), 3.08−3.23 (m, 4H), 3.76 (s, 3H), 6.73 (s, 1H), 7.05−6.90 (m, 2H), 7.71−7.43 (m, 2H), 8.14 (s, 1H), 10.32 (s, 1H), 12.61 (s, 1H). ^{13}C NMR (DMSO-d_6): δ 170.84, 167.70, 159.73, 148.77, 142.53, 126.99, 122.88, 115.02, 93.44, 56.74, 55.87, 54.24, 48.99, 36.22, 35.72, 25.37, 23.25. Mass (ES) m/z: 372 (M + 1). UPLC (acid method); R_t = 0.64 min; area 97%. HRMS: calcd for $C_{19}H_{25}N_5O_3$ + H$^+$, 372.20302; found (ESI, [M + H]$^+$ obsd), 372.20306.

Synthesis of 1-{4-[5-(4-Methoxyphenyl)-2H-pyrazol-3-ylcarbamoyl]butyl}piperidine-4-carboxylic Acid Amide (20). Following the general procedure for 5-aminopentanoic acid amide B1 and starting from commercially available 5-(4-methoxyphenyl)-2H-pyrazol-3-ylamine (**39**, 60 mg, 0.32 mmol), 37 mg of title compound was obtained as formate salt by purification with preparative HPLC (28% yield). ^{1}H NMR (400 MHz, DMSO-d_6): δ 1.42−1.5 (m, 4H), 1.51−1.60 (m, 4H), 1.65−1.69 (m, 2H), 2.01−2.09 (m, 3H), 2.29−2.31 (m, 2H), 2.42−2.55 (m, 2H), 2.97 (m, 2H), 3.75 (s, 3H), 6.73 (s, 1H), 6.97 (d, J = 8.9 Hz, 2H), 7.21 (s, 1H), 7.60 (d, J = 8.8 Hz, 2H), 8.11 (s, 1H), 10.31 (s, 1H). ^{13}C NMR (DMSO-d_6): δ 176.35, 170.79, 164.31, 159.73, 148.20, 142.86, 126.99, 123.10, 115.02, 93.33, 57.25, 55.87, 52.48, 35.74, 35.54, 27.65, 25.15, 23.35. Mass (ES) m/z: 400 (M + 1). UPLC (acid method); R_t = 0.67 min; area 98%. HRMS: calcd for $C_{21}H_{29}N_5O_3$ + H$^+$, 400.23432; found (ESI, [M + H]$^+$ obsd), 400.23394.

Synthesis of 5-[1,4]Oxazepan-4-ylpentanoic Acid [5-(4-Methoxyphenyl)-2H-pyrazol-3-yl] Amide (22). Following the general procedure for 5-aminopentanoic acid amide B1 and starting from commercially available 5-(4-methoxyphenyl)-2H-pyrazol-3-ylamine (**39**, 90 mg, 0.48 mmol), 88 mg of title compound was obtained as formate salt by purification with preparative HPLC (47% yield). ^{1}H NMR (400 MHz, DMSO-d_6): δ 1.32−1.52 (m, 2H), 1.54−1.6 (m, 2H), 1.73−1.77 (m, 2H), 2.26−2.31 (m, 2H), 2.38 −2.55 (m, 2H), 2.56−2.74 (m, 4H), 3.49 −3.73 (m, 4H), 3.78 (s, 3H), 6.73 (s, 1H), 6.98 (d, J = 8.7 Hz, 2H), 7.61 (d, J = 8.7 Hz, 2H), 8.15 (s, 1H), 10.32 (s, 1H), 12.63 (br s, 1H). ^{13}C NMR (CD$_3$OD): δ 171.91, 168.89, 160.22, 146.91, 144.57, 126.68, 122.73, 114.24, 93.20, 67.86, 63.72, 56.88, 56.36, 54.65, 53.13, 35.01, 26.09, 23.90, 22.40. Mass (ES) m/z: 373 (M + 1). UPLC (basic method); R_t = 0.95 min; area 97%. HRMS: calcd for $C_{20}H_{28}N_4O_3$ + H$^+$, 373.22342; found (ESI, [M + H]$^+$ obsd), 373.22346.

Synthesis of 5-[1,4]Diazepan-1-ylpentanoic Acid [5-(4-Methoxyphenyl)-2H-pyrazol-3-yl] Amide (23). Following the general procedure for 5-aminopentanoic acid amide B1 and starting from commercially available 5-(4-methoxyphenyl)-2H-pyrazol-3-ylamine (**39**, 110 mg, 0.58 mmol), 27 mg of title compound was obtained by SiO$_2$ column purification (DCM/MeOH 90:10 to DCM/MeOH NH$_3$ 2 M 80:20) (12% yield). ^{1}H NMR (400 MHz, DMSO-d_6): δ 1.30−1.46 (m, 2H), 1.46−1.60 (m, 2H), 1.72−1.79 (m, 2H), 2.30−2.28 (m, 2H), 2.37−2.46 (m, 2H), 2.53−2.69 (m, 4H), 2.77−3.03 (m, 4H), 3.77 (s, 3H), 4.08 (s, 1H), 6.74 (s, 1H), 6.98 (d, J = 8.8 Hz, 2H), 7.61 (d, J = 8.8 Hz, 2H), 10.31 (s, 1H), 12.59 (s, 1H). ^{13}C NMR (CD$_3$OD): δ 171.83, 160.10, 146.25, 144.37, 126.55, 122.64, 113.24, 93.15, 57.26, 56.45, 56.38, 52.77, 50.15, 50.08, 36.25, 26.21, 23.17, 22.15. Mass (ES) m/z: 372 (M + 1). UPLC (acid method); R_t = 0.82 min; area 95%. HRMS: calcd for $C_{20}H_{29}N_5O_2$ + H$^+$, 372.23940; found (ESI, [M + H]$^+$ obsd), 372.23940.

Synthesis of 5-(5-Oxo[1,4]diazepan-1-yl)pentanoic Acid [5-(4-Methoxyphenyl)-2H-pyrazol-3-yl] Amide (24). Following the general procedure for 5-aminopentanoic acid amide B1 and starting from commercially available 5-(4-methoxyphenyl)-2H-pyrazol-3-ylamine

(**39**, 57 mg, 0.30 mmol), 93 mg of title compound was obtained as the formate salt by purification with preparative HPLC (60% yield). ^{1}H NMR (400 MHz, DMSO-d_6): δ 1.08 (t, J = 12.9 Hz, 1H), 1.39–1.43 (m, 2H), 1.64–1.48 (m, 2H), 2.28 (t, J = 7.3 Hz, 2H), 2.39–2.32 (m, 4H), 2.55–2.41 (m, 2H), 3.01–3.09 (m, 2H), 3.22–3.13 (m, 2H), 3.76 (s, 3H), 6.72 (s, 1H), 7.12–6.84 (m, 2H), 7.49 (s, 1H), 7.68–7.51 (m, 2H), 8.16 (s, 1H), 10.31 (s, 1H). ^{13}C NMR (CD$_3$OD): δ 177.26, 172.26, 166.70, 160.23, 146.99, 144.50, 126.66, 122.71, 114.20, 93.21, 57.60, 56.19, 54.61, 49.91, 39.75, 35.27, 34.72, 24.71, 22.81. Mass (ES) m/z: 386 (M + 1). UPLC (acid method); R_t = 0.63 min; area 98%. HRMS: calcd for C$_{20}$H$_{27}$N$_5$O$_3$ + H$^+$, 386.21867; found (ESI, [M + H]$^+$ obsd), 386.21846.

*5-(4-Acetyl-[1,4]diazepan-1-yl)pentanoic Acid [5-(4-Methoxyphenyl)-1H-pyrazol-3-yl] Amide (**25**).* Following the general procedure for 5-aminopentanoic acid amide B1 and starting from commercially available 5-(4-methoxyphenyl)-2H-pyrazol-3-ylamine (**39**, 1.0 g, 5.56 mmol), 380 mg of title compound was obtained by SiO$_2$ column chromatography (DCM/MeOH 90:10) (14% yield). ^{1}H NMR (400 MHz, DMSO-d_6): δ 1.33–1.45 (m, 2H), 1.49–1.60 (2H, m), 1.62–1.69 (m, 1H), 1.71–1.79 (m, 1H), 1.95 (s, 3H), 2.25–2.33 (m, 2H), 2.35–2.45 (m, 2H), 2.51–2.65 (m, 4H), 3.38–3.47 (m, 4H), 3.77 (s, 3H), 6.77 (bs, 1H), 6.98 (d, J = 8.7 Hz, 2H), 7.61 (d, J = 8.7 Hz, 2H), 10.31 (s, 1H), 12.60 (s, 1H); ^{13}C NMR (CD$_3$OD): δ 172.59, 171.97, 160.22, 147.57, 144.35, 126.65, 122.50, 114.19, 93.28, 57.20, 55.52, 54.60, 54.01, 43.65, 35.57, 26.91, 26.43, 25.87, 23.21, 20.33. Mass (ES) m/z: 414 (M + 1). UPLC (acid method); R_t = 0.69 min; area 100%. HRMS: calcd for C$_{22}$H$_{31}$N$_5$O$_3$ + H$^+$, 414.24997; found (ESI, [M + H]$^+$ obsd), 414.24966.

General Procedure for 5-Aminopentanoic Acid Amide. Route B2, One-Pot Synthesis. To a solution of 5-bromovaleroyl chloride (0.94 mmol, 1 equiv) in DMA (1 mL) cooled at 0 °C was added a solution of 3-amino-5-aryl/heteroaryl heterocycle (0.94 mmol, 1 equiv) and diisopropylethylamine (1.88 mmol, 2 equiv) in DMA (2 mL), and the reaction was stirred for 1 h at 0 °C. The secondary amines (2.35 mmol, 2.5 equiv) and NaI (0.94 mmol, 1 equiv) were then added. The reaction mixture was generally heated at 60 °C for 24−48 h. Upon complete conversion of the bromo-intermediate (as monitored by LC-MS), the solvent was removed under reduced pressure. The residue was taken up in DCM (2 mL) and washed with Na$_2$CO$_3$ saturated water solution. The organic phase was concentrated under reduced pressure and the crude products were either recrystallized from CH$_3$CN or purified by SiO$_2$ column or by preparative HPLC (standard acidic conditions).

*5-Piperidin-1-ylpentanoic Acid [5-(4-Chlorophenyl)-1H-pyrazol-3-yl] Amide (**3**).* Following the general procedure for 5-aminopentanoic acid amide B2 and starting from commercially available 5-(4-chlorophenyl)-1H-pyrazol-3-ylamine (**46**, 187 mg, 0.94 mmol), 40 mg of title compound was obtained by SiO$_2$ (DCM/MeOH 90:10) (10% yield). ^{1}H NMR (400 MHz, DMSO-d_6): δ 1.28–1.56 (m, 10H), 2.20–2.42 (m, 8H), 6.88 (s, 1H), 7.46 (d, J = 8.2 Hz, 2H), 7.69 (d, J = 8.4 Hz, 2H), 10.35 (s, 1H), 12.80 (s, 1H). ^{13}C NMR (CD$_3$OD): δ 171.07, 148.85, 141.29, 133.06, 129.63, 129.63, 127.30, 94.51, 58.44, 54.34, 35.91, 26.05, 25.68, 24.30, 23.62. Mass (ES) m/z: 361 (M + 1). UPLC (basic method); R_t = 1.13; area 98%. HRMS: calcd for C$_{19}$H$_{25}$ClN$_4$O + H$^+$, 361.17897; found (ESI, [M + H]$^+$ obsd), 361.17897.

*Synthesis of 5-Piperidin-1-ylpentanoic Acid [4-(4-Chlorophenyl)-thiazol-2-yl] Amide (**5**).* Following the general procedure for 5-aminopentanoic acid amide B2 and starting from commercially available 4-(4-chlorophenyl)-2H-thiazol-2-ylamine (**38**, 95 mg, 0.45 mmol), 13 mg of title compound was obtained as formate salt by purification with preparative HPLC (9% yield). ^{1}H NMR (400 MHz, CD$_3$OD): δ 1.66 (s, 2H), 1.95–1.72 (m, 8H), 2.58 (t, J = 6.6 Hz, 2H), 3.16–2.95 (m, 3H), 3.30 (dt, J = 3.3, 1.6 Hz, 2H), 7.43–7.27 (m, 3H), 7.94–7.77 (m, 2H), 8.37 (s, 2H). ^{13}C NMR (CD$_3$OD): δ 171.77, 169.11, 158.23, 148.73, 133.49, 133.31, 128.54, 127.30, 107.90, 56.84, 53.17, 34.43, 23.60, 23.33, 22.06, 21.87. Mass (ES) m/z: 378 (M + 1). UPLC (basic method); R_t = 1.50; area 100%. HRMS: calcd for C$_{19}$H$_{24}$ClN$_3$OS + H$^+$, 378.14014; found (ESI, [M + H]$^+$ obsd), 378.13990.

*5-Piperidin-1-ylpentanoic Acid [5-(3-Methoxyphenyl)-2H-pyrazol-3-yl] Amide (**9**).* Following the general procedure for 5-aminopentanoic acid amide B2 and starting from 5-(3-methoxyphenyl)-2H-pyrazol-3-ylamine hydrochloride (**48**, 212 mg, 0.94 mmol), 120 mg of the title compound was isolated by CH$_3$CN wash (35%, yield). ^{1}H NMR (400 MHz, DMSO-d_6): δ 1.29–1.62 (m, 10H), 2.16–2.36 (m, 8H), 3.79 (s, 3H), 6.81–6.93 (m, 2H), 7.26–7.330 (m, 2H), 7.30–7.37 (m, 1H), 10.32 (bs, 1H), 12.76 (bs, 1H). ^{13}C NMR (CD$_3$OD): δ 172.59, 160.43, 144.76, 143.92, 131.55, 129.90, 117.67, 113.93, 110.54, 93.92, 58.88, 54.57, 54.26, 35.77, 25.72, 25.23, 23.98, 23.69. Mass (ES) m/z: 357 (M + 1). UPLC (acid method); R_t = 0.82 min; area 94%. HRMS: calcd for C$_{20}$H$_{28}$N$_4$O$_2$ + H$^+$, 357.22850; found (ESI, [M + H]$^+$ obsd), 357.22839.

*5-Piperidin-1-ylpentanoic Acid [5-(2-Methoxyphenyl)-1H-pyrazol-3-yl] Amide (**10**).* Following the general procedure for 5-aminopentanoic acid amide B2 and starting from 5-(2-methoxyphenyl)-1H-pyrazol-3-ylamine (**49**, 189 mg, 1.0 mmol), 24 mg of the title compound was obtained as the formate salt by preparative HPLC and crystallization with CH$_3$CN (6% yield). ^{1}H NMR (400 MHz, DMSO-d_6): δ 1.34–1.60 (m, 10H), 2.30 (t, J = 6.9 Hz, 2H), 2.46–2.54 (m, 6H), 3.86 (s, 3H), 6.89 (s, 1H), 7.00 (td, J = 7.5, 1.1 Hz, 1H), 7.11 (dd, J = 8.4, 0.9 Hz, 1H), 7.23–7.38 (m, 1H), 7.62 (dd, J = 7.7, 1.6 Hz, 1H), 8.19 (s, 1H), 10.32 (s, 1H), 12.54 (br s, 1H). ^{13}C NMR (CD$_3$OD): δ 171.90, 168.89, 156.46, 146.80, 140.79, 129.64, 127.80, 120.89, 118.05, 111.58, 95.65, 56.70, 54.88, 53.08, 34.97, 23.42, 23.15, 22.37, 21.64. Mass (ES) m/z: 357 (M + 1). UPLC (basic method); R_t = 0.98 min; area 100%. HRMS: calcd for C$_{20}$H$_{28}$N$_4$O$_2$ + H$^+$, 357.22850; found (ESI, [M + H]$^+$ obsd), 357.22831.

*5-Piperidin-1-ylpentanoic Acid [5-(4-Methoxyphenyl)-4-methyl-2H-pyrazol-3-yl] Amide (**11**).* Following the general procedure for 5-aminopentanoic acid amide B2 and starting from 5-(4-methoxyphenyl)-4-methyl-2H-pyrazol-3-ylamine (**44**, 100.0 mg, 0.50 mmol), 53.0 mg of the title compound as the formate salt was obtained as a solid by preparative HPLC (29% yield). ^{1}H NMR (400 MHz, DMSO-d_6): δ 1.30–1.63 (m, 10H), 1.92 (s, 2H), 2.24–2.45 (m, 6H), 3.15 (s, 3H), 3.78 (s, 3H), 7.02 (d, J = 8.8 Hz, 2H), 7.47 (d, J = 8.8 Hz, 2H), 8.19 (s, 1H), 9.57 (s, 1H), 12.51 (br s, 1H). ^{13}C NMR (CD$_3$OD): δ 174.12, 159.99, 152.03, 139.95, 128.50, 123.34, 114.12, 92.30, 58.26, 54.64, 53.94, 35.22, 25.07, 24.64, 23.43, 23.30, 7.65. Mass (ES) m/z: 371 (M + 1). UPLC (basic method); R_t = 0.96 min; area 100%. HRMS: calcd for C$_{21}$H$_{30}$N$_4$O$_2$ + H$^+$, 371.24415; found (ESI, [M + H]$^+$ obsd), 371.24384.

*5-Piperidin-1-ylpentanoic Acid [5-(4-Fluorophenyl)-2H-pyrazol-3-yl] Amide (**12**).* Following the general procedure for 5-aminopentanoic acid amide B2 and starting from commercially available 5-(4-fluorophenyl)-2H-pyrazol-3-ylamine (**42**, 0.35 g, 2.00 mmol), 87.4 mg of title compound as the formate salt was obtained as a solid by preparative HPLC (19%, yield). ^{1}H NMR (400 MHz, DMSO-d_6): δ 1.32–1.61 (m, 10H), 2.30 (t, J = 7.0 Hz, 2H), 2.46–2.57 (m, 6H), 6.79 (s, 1H), 7.26 (t, J = 8.9 Hz, 2H), 7.82–7.64 (m, 2H), 8.23 (s, 1H), 8.23 (s, 1H), 12.49 (brs, 1H). ^{13}C NMR (CD$_3$OD): δ 171.90, 169.08, 162.93 (d, J = 246.6 Hz), 146.47, 144.17, 127.39, 126.92, 115.67 (d, J = 22.1 Hz), 93.59, 56.61, 52.96, 34.98, 23.36, 23.08, 22.39, 21.66. Mass (ES) m/z: 345 (M + 1). UPLC (acid method); R_t = 0.82 min; area 98%. HRMS: calcd for C$_{19}$H$_{25}$FN$_4$O + H$^+$, 345.20852; found (ESI, [M + H]$^+$ obsd), 345.20835.

*5-Piperidin-1-ylpentanoic Acid [5-(4-Bromophenyl)-2H-pyrazol-3-yl] Amide (**13**).* Following the general procedure for 5-aminopentanoic acid amide B2 and starting from commercially available 5-(4-bromophenyl)-2H-pyrazol-3-ylamine (**43**, 0.50 g, 2.10 mmol), 230.0 mg of the title compound was obtained by crystallization with ethyl acetate (27% yield). ^{1}H NMR (400 MHz, DMSO-d_6): δ 1.30–1.42 (m, 1H), 1.53–1.71 (m, 7H), 1.74–1.83 (m, 2H), 2.31–2.39 (m, 2H), 2.77–2.79 (m, 2H), 2.97–3.04 (m, 2H), 3.36–3.45 (m, 2H), 6.91 (s, 1H), 7.64 (s, 4H), 8.84 (s, 1H), 12.87 (s, 1H). ^{13}C NMR (DMSO-d_6): δ 170.52, 148.89, 141.14, 132.61, 129.16, 127.59, 121.79, 94.63, 56.16, 52.66, 35.36, 23.57, 23.21, 22.80, 21.94. Mass (ES) m/z: 405 (M + 1). UPLC (acid method); R_t = 1.03 min; area 100%. HRMS: calcd for C$_{19}$H$_{25}$BrN$_4$O + H$^+$, 405.12845; found (ESI, [M + H]$^+$ obsd), 405.12861.

5-Piperidin-1-ylpentanoic Acid (5-Pyridin-4-yl-1H-pyrazol-3-yl) Amide (14). Following the general procedure for 5-aminopentanoic acid amide B2 and starting from 5-pyridin-4-yl-1H-pyrazol-3-ylamine (**45**, 151 mg, 0.94 mmol) and piperidine as secondary amine, 30 mg of title compound was obtained by SiO₂ column chromatography (10% yield). ¹H NMR (400 MHz, DMSO-d_6): δ 1.33−1.60 (m, 10H), 2.28−2.48 (m, 8H), 7.03 (bs, 1H), 7.68 (dd, J = 4.6, 1.6 Hz, 2H), 8.59 (d, J = 6.0 Hz, 2H), 10.49 (s, 1H), 13.11 (s, 1H). ¹³C NMR (DMSO-d_6): δ 171.15, 150.99, 147.92, 141.31, 137.56, 119.78, 95.08, 58.27, 54.22, 35.85, 25.87, 25.51, 24.15, 23.54. Mass (ES) m/z: 328 (M + 1). UPLC (basic method); R_t = 0.61 min; area 100%. HRMS: calcd for C₁₈H₂₅N₅O + H⁺, 328.21319; found (ESI, [M + H]⁺ obsd), 328.21307.

5-Piperidin-1-ylpentanoic Acid [5-(4-Trifluoromethylphenyl)-1H-pyrazol-3-yl] Amide (15). Following the general procedure for 5-aminopentanoic acid amide B2 and starting from 5-(4-trifluoromethylphenyl)-1H-pyrazol-3-ylamine (**47**, 214 mg, 0.94 mmol), 30 mg of title compound was obtained by SiO₂ (DCM/MeOH 90:10) (10%, yield). ¹H NMR (400 MHz, DMSO-d_6): δ 1.29−1.59 (m, 10H), 2.15−2.33 (m, 8H), 6.98 (s, broad, 1H), 7.76 (d, J = 8.5 Hz, 2H), 7.91 (d, J = 7.9 Hz, 2H), 10.42 (s, 1H), 12.97 (s, 1H). ¹³C NMR (DMSO-d_6) δ 171.25, 156.11, 141.54, 136.36, 128.92−128.23 (m), 126.52, 126.13, 124.87 (q, J = 271.5 Hz), 94.82, 58.96, 54.73, 36.03, 26.63, 26.26, 24.85, 23.80. Mass (ES) m/z: 395 (M + 1). UPLC (basic method); R_t = 1.25 min; area 100%. HRMS: calcd for C₂₀H₂₅F₃N₄O + H⁺, 395.20532; found (ESI, [M + H]⁺ obsd), 395.20503.

5-Piperidin-1-ylpentanoic Acid (5-Furan-2-yl-2H-pyrazol-3-yl) Amide (16). Following the general procedure for 5-aminopentanoic acid amide B2 and starting from commercially available 5-furan-2-yl-2H-pyrazol-3-ylamine (**41**, 0.30 g, 2.03 mmol), 96.0 mg of title compound was obtained as the formate salt as a solid by preparative HPLC (15%, yield). ¹H NMR (400 MHz, CD₃OD): δ 1.54−1.94 (m, 10H), 2.48 (t, J = 6.7 Hz, 2H), 3.05−3.12 (m, 2H), 3.00−3.39 (m, 4H), 6.52 (dd, J = 3.4, 1.8 Hz, 1H), 6.66 (s, 1H), 6.70 (d, J = 3.4 Hz, 1H), 7.56 (d, J = 1.7 Hz, 1H), 8.48 (s, 1H). ¹³C NMR (CD₃OD): δ 171.86, 169.12, 146.15, 145.89, 142.61, 136.72, 111.40, 106.48, 92.77, 56.63, 52.99, 34.98, 23.38, 23.10, 22.37, 21.66. Mass (ES) 317 m/z: (M + 1). UPLC (basic method); R_t = 0.76 min; area 100%. HRMS: calcd for C₁₇H₂₄N₄O₂ + H⁺, 317.19720; found (ESI, [M + H]⁺ obsd), 317.19716.

5-Morpholin-4-ylpentanoic Acid [5-(4-Methoxyphenyl)-1H-pyrazol-3-yl] Amide (18). Following the general procedure for 5-aminopentanoic acid amide B2 and starting from the commercially available 5-(4-methoxyphenyl)-2H-pyrazol-3-ylamine (**39**, 568 mg, 3 mmol), 110 mg of the title compound as the formate salt was obtained by purification with preparative HPLC (10% yield). ¹H NMR (400 MHz, DMSO-d_6): δ 1.38−1.47 (m, 2H), 1.51−1.61 (m, 2H), 2.23−2.35 (m, 8H), 3.51−3.56 (m, 4H), 3.76 (s, 3H), 6.73 (s, 1H), 6.98 (d, J = 8.7 Hz, 2H), 7.61 (d, J = 8.8 Hz, 2H), 8.13 (s, 1H), 10.31 (s, 1H), 12.76 (br s, 1H). ¹³C NMR (DMSO-d_6): δ 170.99, 163.99, 159.72, 148.20, 142.79, 126.98, 123.09, 115.01, 93.32, 66.70, 58.46, 55.85, 53.87, 35.94, 25.99, 23.64. Mass (ES) m/z: 359 (M + 1). UPLC (basic method); R_t = 1.0 min; area 95%. HRMS: calcd for C₁₉H₂₆N₄O₃ + H⁺, 359.20777; found (ESI, [M + H]⁺ obsd), 359.20785.

Synthesis of 5-Azepan-1-ylpentanoic Acid [5-(4-Methoxyphenyl)-2H-pyrazol-3-yl] Amide (21). Following the general procedure for 5-aminopentanoic acid amide B2 and starting from the commercially available 5-(4-methoxyphenyl)-2H-pyrazol-3-ylamine (**39**, 89 mg, 0.45 mmol), 46 mg of title compound as the formate salt was obtained by purification with preparative HPLC (27% yield). ¹H NMR (400 MHz, CD₃OD): δ 1.69−1.96 (m, 12H), 2.49 (t, J = 7.2 Hz, 2H), 3.15−3.21 (m, 2H), 3.28−3.35 (m, 4H), 3.83 (s, 3H), 6.70 (s, 1H), 6.99 (d, J = 8.8 Hz, 2H), 7.59 (d, J = 8.8 Hz, 2H), 8.46 (s, 1H). ¹³C NMR (CD₃OD): δ 171.92, 169.00, 160.25, 146.96, 144.43, 126.64, 122.67, 114.21, 93.22, 57.10, 54.66, 54.62, 34.90, 26.23, 23.82, 23.69, 22.28. Mass (ES) m/z: 371 (M + 1). UPLC (basic method); R_t = 1.0 min; area 95%. HRMS: calcd for C₂₁H₃₀N₄O₂ + H⁺, 371.24415; found (ESI, [M + H]⁺ obsd), 371.24407.

5-(4-Acetyl[1,4]diazepan-1-yl)pentanoic Acid [5-(4-Methoxyphenyl)-4-methyl-2H-pyrazol-3-yl] Amide (26). Following the

general procedure for 5-aminopentanoic acid amide B2 and starting from 5-(4-methoxyphenyl)-4-methyl-2H-pyrazol-3-ylamine (**44**, 100.0 mg, 0.50 mmol), 34.0 mg of title compound was obtained by SiO₂ column purification (DCM/MeOH 90:10 to DCM/MeOH NH₃ 2 M 80:20) (12% yield). (16% yield). ¹H NMR (400 MHz, CD₃OD): δ 1.43−1.62 (m, 4H), 1.67−1.77 (m, 1H), 1.80−1.88 (m, 1H), 1.92 (s, 3H), 1.98 (s, 3H), 2.26−2.34 (m, 2H), 2.53−2.70 (m, 3H), 2.72−2.83 (m, 3H), 3.40−3.54 (m, 4H), 3.78 (s, 3H), 7.02 (d, J = 8.8 Hz, 2H), 7.47 (d, J = 8.7 Hz, 2H), 8.12 (s, 1H), 9.58 (s, 1H). ¹³C NMR (CD₃OD): δ 172.28, 168.73, 160.02, 144.12, 142.15, 128.50, 123.11, 114.12, 106.62, 57.13, 55.31, 54.62, 53.67, 43.68, 41.48, 34.82, 25.56, 24.64, 22.75, 20.44, 7.60. Mass (ES) m/z: 428 (M + 1). UPLC (basic method); R_t = 0.96 min; area 100%. HRMS: calcd for C₂₃H₃₃N₅O₃ + H⁺, 428.26562; found (ESI, [M + H]⁺ obsd), 428.26532.

Procedure for 5-(4-Acetyl[1,4]diazepan-1-yl)-2-methylpentanoic Acid [5-(4-Methoxyphenyl)-2H-pyrazol-3-yl] Amide (27). Route C. 5-Amino-3-(4-methoxyphenyl)pyrazole-1-carboxylic Acid tert-Butyl Ester (54). To a vigorously stirred solution of commercially available 5-(4-methoxyphenyl)-2H-pyrazol-3-ylamine (**39**, 500 mg, 2.64 mmol) in DCM (20 mL) was added an aqueous solution of 4.5 N KOH (4.7 mL, 21.1 mmol), followed by di-*tert*-butyl dicarbonate (605 mg, 2.77 mmol). The mixture was stirred for 20 h, and then 20 mL of water was added and the organic phase was collected and the solvent was removed under reduced pressure. The crude was purified by SiO₂ column chromatography, eluting with DCM, affording 720 mg of the title product. ¹H NMR (400 MHz, DMSO-d_6): δ 1.57 (s, 9H), 3.77 (s, 3H), 5.68 (s, 1H), 6.34 (bs, 2H), 6.95 (d, J = 7.8 Hz, 2H), 7.67 (d, J = 7.8 Hz, 2H). Mass (ES) m/z: 290 (M + 1).

2-(3-Bromopropyl)-2-methylmalonic Acid (52). NaH (60% mineral oil dispersion, 3.25 g, 81 mmol) was placed in a flask under inert atmosphere, anhydrous THF (60 mL) was added, and the mixture was cooled down to 0 °C. A solution of 2-methylmalonic acid dimethyl ester (**50**, 9.9 g, 67.7 mmol) in THF (15 mL) was added dropwise, and the reaction was left stirring at 0 °C for 15 min. 1,3-Dibromopropane (**51**, 47.8 g, 237 mmol) was added in one portion, and after 15 min the reaction was allowed to warm up to room temperature and left stirring for 18 h. 1 N NaOH solution was carefully added, and the product was extracted with ethyl acetate. The organic phase was collected and the solvent removed under reduced pressure; the crude was purified by SiO₂ column chromatography (cyclohexane/ethyl acetate 50:50), affording 15.1 g of the title compound (84%, yield). ¹H NMR (400 MHz, DMSO-d_6): δ 1.32 (s, 3H), 1.64−1.75 (m, 2H), 1.85−1.93 (m, 2H), 3.51 (t, J = 6.2 Hz, 2H), 3.64 (s, 6.2H).

5-Bromo-2-methylpentanoic Acid (53). 2-(3-Bromopropyl)-2-methylmalonic acid (**53**, 10 g, 37.4 mmol) was mixed with 48% aqueous HBr (80 mL, 589 mmol), and the mixture was heated at 110 °C for 24 h. The mixture was allowed to cool down to room temperature and then to 0 °C. 100 mL of H₂O and NaOH (22 g, 550 mml) was carefully added, and the product was extracted with 200 mL of a mixture of DCM/MeOH (95:5). The organic phase was collected and the solvent removed under reduced pressure, affording 6.6 g of title compound (84%, yield). ¹H NMR (400 MHz, DMSO-d_6): δ 1.03 (d, J = 7.1 Hz, 3H), 1.38−1.48 (m, 1H), 1.58−1.60 (m, 1H), 1.72−1.82 (m, 2H), 2.26−2.38 (m, 1H), 3.50 (t, J = 7.8 Hz, 2H), 12.13 (bs, 1H).

5-[5-(4-Acetyl[1,4]diazepan-1-yl)-2-methylpentanoylamino]-3-(4-methoxyphenyl)pyrazole-1-carboxylic Acid tert-Butyl Ester (56). To a solution of 5-bromo-2-methylpentanoic acid (**53**, 330 mg, 1.70 mmol) in DCM (1 mL) was added oxalyl chloride (219 μL, 2.55 mmol), and the mixture was stirred for 2 h under nitrogen flow. Solvent and excess oxalyl chloride were removed under reduced pressure. The residue was dissolved in 1 mL of DCM and added dropwise to a solution of 5-amino-3-(4-methoxyphenyl)pyrazole-1-carboxylic acid *tert*-butyl ester (**54**, 490 mg, 1.70 mmol) and triethylamine (236 μL, 1.70 mmol) in DCM (3 mL). The mixture was stirred at room temperature for 48 h. NaHCO₃ saturated solution was added, the organic phase was collected, and the solvent was removed under reduced pressure. 5-(5-Bromo-2-methylpentanoylamino)-3-(4-methoxyphenyl)pyrazole-1-carboxylic acid *tert*-butyl ester

(**55**, 442 mg) was obtained after SiO$_2$ column chromatography (DCM/cyclohexane 50:50).

Triethylamine (80 μL, 0.6 mmol) and *N*-acetyl diazepine (158 μL, 0.6 mmol) were added to a solution of 5-(5-bromo-2-methylpentanoylamino)-3-(4-methoxyphenyl)pyrazole-1-carboxylic acid *tert*-butyl ester (**55**, 280 mg, 0.6 mmol) in DCM. The reaction mixture was stirred for 24 h at room temperature and then for 15 h at 50 °C. NaHCO$_3$ saturated solution was added, the organic phase was collected, and the solvent was removed under reduced pressure. The crude was purified by SiO$_2$ column chromatography (DCM/MeOH, 98:2), affording 181 mg of the title compound (57%, yield). ^{1}H NMR (400 MHz, DMSO-d_6): δ 1.08 (m, 5H), 1.31−1.50 (m, 3H), 1.60 (s, 9H), 1.69−1.81 (m, 1H), 1.92−1.98 (m, 3H), 2.33−2.44 (m, 2H), 2.50−2.71 (m, 2H), 2.96−3.11 (m, 2H), 3.37−3.53 (m, 5H), 3.78 (s, 3H), 6.99 (d, J = 8.7 Hz, 2H), 7.04 (bs, 1H), 7.77 (d, J = 8.7 Hz, 2H), 10.04 (bs, 1H).

5-(4-Acetyl[1,4]diazepan-1-yl)-2-methylpentanoic Acid [5-(4-Methoxyphenyl)-2H-pyrazol-3-yl] Amide (27). 5-[5-(4-Acetyl[1,4]-diazepan-1-yl)-2-methylpentanoylamino]-3-(4-methoxyphenyl)-pyrazole-1-carboxylic acid *tert*-butyl ester (**56**, 181 mg, 0.344 mmol) was dissolved in 3 mL of DCM, and a solution of 4 N HCl in dioxane (0.16 mL, 0.648 mmol) was added. The mixture was stirred for 3 h at room temperature, and then NaHCO$_3$ saturated solution was added, the organic phase was collected, and the solvent removed under reduced pressure. 150 mg of the title compound was isolated (82%, yield).

^{1}H NMR (400 MHz, DMSO-d_6): δ 1.03 (d, J = 6.6 Hz, 3H), 1.22−1.43 (m, 3H), 1.46−1.59 (m, 1H), 1.59−1.68 (m, 1H), 1.68−1.77 (m, 1H), 1.95 (s, 3H), 2.32−2.42 (m, 2H), 2.45−2.53 (m, 2H), 2.55−2.63 (m, 2H), 3.29−3.46 (m, 5H), 3.76 (s, 3H), 6.78 (bs, 1H), 6.98 (d, J = 8.7 Hz, 2H), 7.61 (d, J = 8.7 Hz, 2H), 10.30 (bs, 1H), 12.61 (br s, 1H). ^{13}C NMR (CD$_3$OD): δ 176.09, 171.89, 160.20, 147.33, 144.18, 126.66, 122.70, 114.21, 93.49, 57.42, 55.51, 54.62, 54.09, 44.25, 44.05, 40.79, 31.91, 27.25, 24.74, 20.41, 17.32. Mass (ES) m/z: 428 (M + 1). UPLC (basic method); R_t = 1.02; area 100%. HRMS: calcd for C$_{23}$H$_{33}$N$_5$O$_3$ + H$^+$, 428.26562; found (ESI, [M + H]$^+$ obsd), 428.26549.

General Procedure for 3-Amino-5-aryl/Heteroaryl Pyrazole. Route D1. To a solution of an aryl or heteroaryl methyl carboxylate (6.5 mmol) in dry toluene (6 mL) under N$_2$ was carefully added NaH (50−60% dispersion in mineral oil, 624 mg, 13 mmol). The mixture was heated at 80 °C, and then dry CH$_3$CN was added dropwise (1.6 mL, 30.8 mmol). The reaction was heated for 18 h, and generally the product precipitated from the reaction mixture as the Na salt.

The reaction was then allowed to cool down to room temperature, and the solid formed was filtered and then dissolved in water. The solution was then acidified with 2 N HCl solution, and at pH between 2 and 6 (depending on the ring substitution on the aryl/heteroaryl system) the product precipitated and was filtered off. If no precipitation occurred, the product was extracted with DCM.

After workup, the products were generally used in the following step without further purification. The general yield was between 40 and 80%.

To a solution of the β-ketonitrile (7.5 mmol) in absolute EtOH (15 mL) was added hydrazine monohydrate (0.44 mL, 9.0 mmol), and the reaction was heated at reflux for 18 h. The reaction mixture was allowed to cool down to room temperature, and the solvent was evaporated under reduced pressure. The residue was dissolved in DCM and washed with water.

The organic phase was concentrated under reduced pressure to give a product that, if not pure enough, was purified by SiO$_2$ column or by precipitation from Et$_2$O. Yields were generally between 65 and 90%.

5-(4-Methoxyphenyl)-4-methyl-2H-pyrazol-3-ylamine (44). Following the general procedure for 3-amino-5-aryl/heteroaryl pyrazole D1 and starting from commercially available 4-methoxybenzoic acid methyl ester (3.0 mL, 18.0 mmol) were obtained 2.1 g of title compound by column chromatography (DCM/MeOH 90:10) (62% yield). ^{1}H NMR (400 MHz, CDCl$_3$): δ 2.03 (s, 3H), 3.58 (brs, 2H), 3.84 (s, 3H), 6.96−6.98 (m, 2H), 7.37−7.39 (m, 2H). Mass (ES) m/z: 204 (M + 1).

General Procedure for 3-Amino-5-aryl/Heteroaryl Pyrazole. Route D2. To a solution of dry alkanenitrile in toluene (1 mmol/mL, 5 equiv) cooled down to −78 °C under nitrogen was added dropwise a solution of *n*-butyllithium in *n*-hexane (1.6 N, 3.5 equiv). The mixture was left stirring at −78 °C for 20 min, and then a solution of the aryl or heteroaryl methyl carboxylate in toluene (0.75 mmol/mL, 1 equiv) was added and the reaction was allowed to reach room temperature. Upon reaction completion, after about 20 min, the mixture was cooled down to 0 °C and HCl 2 N was added to pH 2. The organic phase was recovered, dried over Na$_2$SO$_4$, and concentrated under reduced pressure, affording the title product, which was generally used without further purification.

To a solution of the β-ketonitrile (7.5 mmoL), in absolute EtOH (15 mL), was added hydrazine monohydrate (0.44 mL, 9.0 mmol), and the reaction was heated at reflux for 18 h. The reaction mixture was allowed to cool to room temperature, and the solvent was evaporated under reduced pressure. The residue was dissolved in DCM and washed with water.

The organic phase was concentrated under reduced pressure to give a product that, if not pure enough, was purified by SiO$_2$ column or by precipitation from Et$_2$O. Yields were generally between 65 and 90%.

5-Pyridin-4-yl-2H-pyrazol-3-ylamine (45). Following the general procedure for 3-amino-5-aryl/heteroaryl pyrazole D2 and starting from commercially available isonicotinic acid methyl ester (3.0 g, 21.9 mmol), 1.8 g of the title compound was obtained (40% yield). ^{1}H NMR (400 MHz, DMSO-d_6): δ 5.00 (bs, 2H), 5.85 (s, 1H), 7.59 (dd, J = 4.6, 1.6 Hz, 2H), 8.50 (d, J = 6.0 Hz, 2H), 11.83 (s, 1H). Mass (ES) m/z: 161 (M + 1).

5-(4-(Trifluoromethyl)phenyl)-2H-pyrazol-3-ylamine (47). Following the general procedure for 3-amino-5-aryl/heteroaryl pyrazole D2 and starting from commercially available 4-trifluoromethylbenzoic acid methyl ester (5.0 g, 3.94 mL, 24.5 mmol), 5.35 g of the title compound was obtained (40% yield). ^{1}H NMR (400 MHz, DMSO-d_6): δ 5.10 (s, broad, 2H), 5.77 (s, 1H), 7.68 (d, J = 7.1 Hz, 2H), 7.85 (d, J = 8.0 Hz, 2H), 11.92 (bs, 1H). Mass (ES) m/z: 228 (M + 1).

5-(3-Methoxyphenyl)-2H-pyrazol-3-ylamine (48). Following the general procedure for 3-amino-5-aryl/heteroaryl pyrazole D2 and starting from commercially available 3-methoxybenzoic acid methyl ester (2.98 g, 18.0 mmol), 1.8 g of title compound was obtained by precipitation with Et$_2$O (42% yield). ^{1}H NMR (400 MHz, CDCl$_3$): δ 3.78 (s, 3H), 4.97 (bs, 4H), 5.87 (s, 1H), 6.81−6.88 (m, 1H), 7.07−7.16 (m, 1H), 2.23−7.31 (m, 1H). Mass (ES) m/z: 190 (M + 1).

5-(2-Methoxyphenyl)-2H-pyrazol-3-ylamine (49). Following the general procedure for 3-amino-5-aryl/heteroaryl pyrazole D2 and starting from commercially available 3-methoxybenzoic acid methyl ester (2.5 mL, 18.0 mmol). 1.40 g of the title compound was obtained by precipitation from Et$_2$O (42% yield). ^{1}H NMR (400 MHz, CD$_3$OD): δ 3.82 (s, 3H), 5.92 (bs, 1H), 6.85−6.90 (m, 1H), 7.16−7.33 (m, 3H). Mass (ES) m/z: 190 (M + 1).

3. Biology. Ca^{2+}-Flux and Membrane Potential Measurements with a Fluorescence Imaging Plate Reader. The following recombinant cell lines were used as specific sources of receptors: GH4C1 cells stably transfected with pCEP4/rat α7 nAChR as previously described,[35] HEK293 cell lines stably expressing human 5-HT3A receptors.[35] Native neuroblastoma SH-SY5Y cells were used as a source of human ganglionic nAChRs (α3), and TE671 rhabdomyosarcoma cells were used as an endogenous source of muscle α1β1δγ receptors. GH4C1 cells expressing α7 and HEK cells expressing 5-HT3A receptors were analyzed by Ca^{2+}-flux measurements employing a fluorometric imaging plate reader (FLIPR, Molecular Devices) system, whereas the cells expressing the nicotinic receptor subunits α1 and α3 were tested in the FLIPR system with a membrane potential sensitive dye. For Ca^{2+}-flux analysis, cells were plated in 96-well clear-bottom, poly D-lysine coated black microtiter plates (Costar) at a density of 1 × 10^5 cells/well for α7 expressing GH4C1 cells or 8 × 10^4 cells/well for 5-HT3A expressing HEK293 cells and cultured for 24 h prior to experiments. The medium was then replaced with 100 μL of Hank's balanced salt solution-HEPES 20 mM, pH 7.4 (assay buffer) containing 4 μM Fluo-4 a.m., 0.02% pluronic acid, and 5 mM probenecid. After 40 min of incubation at 37 °C, the

labeling solution was replaced with 200 μL of assay buffer containing 2.5 mM probenecid. Plates were then transferred to the FLIPR system. Compounds to be tested were prepared in assay buffer as 5×-concentrated solutions in a separate 96-well polypropylene plate. Basal fluorescence was recorded for 30 s, followed by addition of 50 μL of test compound (to assess agonist activity; first addition). Measurements were made at 1 s intervals for 1 min, followed by measurements every 30 s for 10 min. Subsequently, for the second addition for alpha-7 expressing GH4C1 cells, nicotine was added to each well except negative controls at the EC$_{80}$ final concentration to assess the antagonism of the nicotine response or at the EC$_{20}$ final concentration to assess the positive modulation of the nicotine response. Assay performance was robust, as reflected by a Z′ factor > 0.6. For testing 5-HT3A receptor activity, m-chlorophenylbiguanide (CPBG, EC$_{80}$ final concentration) was added to each well except negative controls. Measurements were made at 1 s intervals for 1 min after the second addition and at 3 s intervals for the remaining 3 min. Results were exported from the FLIPR raw data as MAX-MIN of the fluorescence signal intensity in two intervals corresponding to the first and the second addition of compounds. The responses were normalized to the positive control and EC$_{50}$ and IC$_{50}$ values were calculated using XlFit version 4.2, with a sigmoidal concentration–response (variable slope) equation: $Y = \text{bottom} + (\text{top} - \text{bottom})/(1 + (\text{EC}_{50}/X)^{\text{Hill Slope}})$, where X was the concentration, Y was the response, bottom was the bottom plateau of the curve, and top was the top plateau. The activity of compounds at the muscle and ganglionic type nAChR receptors was determined using a membrane potential sensitive fluorescent dye. TE671 and SHSY5Y cells were plated at a density of 5×10^4 and 1×10^5 cells/well, respectively, 24 h prior to assay. Growth media were removed from the cells by flicking the plates, and membrane potential dye (Molecular Devices), reconstituted in HBSS five times more diluted compared to the manufacturer's instructions, was added to the wells. Plates were incubated for 60 min at room temperature and then directly transferred to the FLIPR system. Compounds to be tested were prepared in assay buffer as 5×-concentrated solutions in a separate 96-well polypropylene plate. Baseline fluorescence was monitored for the first 10 s followed by the addition of compounds. For detection of antagonist activity, agonist (epibatidine; EC$_{80}$ final concentration) was added to every well except negative controls. Signal recordings were performed as above. Results for SH-SY5Y cells were exported as described previously whereas for TE671 were exported from the FLIPR raw data as SUM of fluorescence signal intensity for the first addition and MAX-MIN for the second addition of compounds. The responses were normalized to the positive control (epibatidine 1 μM final concentration). The compounds tested were found to display antagonist activity, and IC$_{50}$ values were calculated as described before.

Solubility Assay. Standard and sample solutions were prepared from a 10 mM DMSO stock solution using an automated dilution procedure. For each compound, three solutions were prepared: one to be used as standard and the other two as test solutions. Standard: 250 μM standard solution in acetonitrile/buffer, with a final DMSO content of 2.5% (v/v). Test sample for pH 3.0: 250 μM sample solution in acetic acid 50 mM, pH = 3, with a final DMSO content of 2.5% (v/v). Test sample for pH 7.4: a 250 μM sample solution in ammonium acetate buffer 50 mM, pH = 7.4, with a final DMSO content of 2.5% (v/v). The 250 μM product suspensions/solutions in the aqueous buffers were prepared directly in Millipore MultiScreen-96 filter plates (0.4 μm PTCE membrane) and sealed. Plates were left for 24 h at room temperature under orbital shaking to achieve "pseudo-thermodynamic equilibrium" and to presaturate the membrane filter. Product suspensions/solutions were then filtered using centrifugation, diluted 1:2 with the same buffer solution, and analyzed by UPLC/UV/TOF-MS, using UV detection at 254 nm for quantitation. Solubility was calculated by comparing the sample and standard UV areas: $S = (A_{\text{smp}} \times \text{FD} \times C_{\text{st}})/A_{\text{st}}$, where S was the solubility of the compound (μM), A_{smp} was the UV area of the sample solution, FD was the dilution factor (2), C_{st} was the standard concentration (250 μM), and A_{st} was the UV area of the standard solution.

Cytochrome P450 Inhibition Assay..[36,37] The fluorescent P450 inhibition assay was performed using the Gentest method (http://www.gentest.com). Test compounds were dissolved in DMSO at 1.5 mM. The stock solution of 12 μL was added by a robotic system to 1488 μL of 0.1 M phosphate buffer at pH 7.4. The solution was mixed, and 50 μL of the diluted samples was added to a 1 mL 96-well polypropylene plate. Then 50 μL of cofactor with a NADPH regenerating system was added to the wells. The plate was incubated at 37 °C for 10 min. Enzyme–substrate mix was prepared by prewarming the buffer at 37 °C for at least 10 min, and the enzymes and substrates were added right before addition to the reaction plate. Enzyme–substrate mix (100 μL) was added to the wells to start the reaction. The final substrate and isozyme concentrations and incubation time were as follows: BFC (50 μM)/CYP3A4 (5 pmol/mL) for 30 min, AMMC (1.5 μM)/CYP2D6 (7.5 pmol/mL) for 30 min, and MFC (75 μM)/2C9 (20 pmol/mL) for 45 min. The reactions were stopped with 80% ACN/20% 0.5 M Tris buffer. The signals were quantified using a fluorescent plate reader. The final DMSO concentration was 0.2%. Compounds were tested in duplicate. Percent inhibition was determined at 3 μM compound concentration. High negative values were usually indicative of fluorescent interference from the test compounds or metabolites. The % CV obtained was typically within 10%.

Metabolic Stability Assay. Compounds in 10 mM DMSO solution were added to an incubation mixture in a 96-well microplate containing 20 pmol/mL of hCYP3A4. The mixture was split in two aliquots: one receiving a NADPH regenerating system, the other an equal amount of phosphate buffer. The final substrate concentration was 1 μM along with 0.25% of organic solvent. Incubation proceeded for 1 h at 37 °C and was stopped by addition of acetonitrile to precipitate proteins. Metabolic stability was given as the percent remaining following incubation with cofactor (NADPH) with reference to the incubation mixture without NADPH: % remaining = area NADPH × 100/area ctrl where area ctrl was the MS peak area of the sample solution without NADPH and area NADPH was the MS area of the sample solution with NADPH. The % CV obtained was typically within 10%.

Permeability Assay. The assay was run in a PAMPA filter plate, and compounds (10 μM in HBSS + Hepes buffer pH = 7.4) were added to the donor chamber and incubated for 4 h at 37 °C and 80% humidity. Warfarin was used in each well as control for membrane integrity. Concentrations of reference $t(0)$, donor, and acceptor solutions were measured by UPLC-MS-TOF. The passive permeability was calculated according to the following expression[38]

$$CA(t) = \left(\frac{M}{V_D + V_A}\right) + \left(CA(0) - \frac{M}{V_D + V_A}\right)e^{-P_eA\left(\frac{1}{V_D} + \frac{1}{V_A}\right)t}$$

where M refers to the total amount of drug in the system minus the amount of sample lost in membrane (and surfaces), $CA(t)$ was the concentration of the drug in the acceptor well at time t, $CA(0)$ was the concentration of the drug in the acceptor well at time 0, V_A was the volume of the acceptor well, V_D was the volume of the donor well, P_e was the effective permeability, A was the membrane area, and t was the permeation time. Compounds were defined as low, medium, or highly permeable following the following classification: $>10 \times 10^{-6}$ cm/s, high (passive permeability was unlikely to be limiting for passive diffusion); between 2 and 10×10^{-6} cm/s, medium (permeability may be limiting in the case of low solubility, high metabolic turnover rate or active secretion); between 0 and 2×10^{-6} cm/s, low (high risk that permeability was limiting for passive diffusion).

In Vitro Intrinsic Clearance. Test compounds were incubated separately at 1 μM concentration in 100 mM phosphate buffer (pH 7.4) and 1 mM EDTA with 0.2 mg/mL rat hepatic microsomal protein. The enzymatic reaction was initiated by addition of a NADPH regenerating system (final concentrations: 2 mM ß-nicotinamide adenine dinucleotide phosphate (NADP) + 10 mM glucose-6-phosphate (G6P) + 0.4 U/mL glucose-6-phosphate dehydrogenase (G6PDH)). Reactions were terminated at regular time intervals (0–5–10–20–40 min) by adding an equal volume of acetonitrile. All

incubations were performed in duplicate. Verapamil as positive control for the assay was incubated in parallel under the same conditions. Samples were analyzed by UPLC/TOF-MS. Quantitative data were automatically produced using the OpenLynx software. Substrate depletion data (peak area at different time points) were fitted to a monoexponential decay model (eq 1), with a $1/y$ weighting, $C_{(t)} = C_0 e^{-kt}$, where C_0 was the substrate concentration in the incubation media at time 0 and k was the terminal rate constant. Under the assumption that the concentration of 1 μM was far below the K_m of the test compound, the in vitro Cl_{int} was calculated by dividing the elimination constant (K) for the microsomal protein concentration (PMS), expressed in mg/μL, to obtain Cl_{int} in units of μL/min/mg protein: $Cl_{int} = K/PMS = \mu L/min/mg$ protein. Compounds were defined as low, medium, or highly metabolized based on the in vitro Cl_{int} values: <3.4, low; 3.4−92.4, mediun; >92.4, high.

Plasma Stability. Fresh plasma (no more than 2−4 h from a blood draw), spiked with a 250 μM solution of test item dissolved in acetonitrile 12%, was divided into three aliquots (one for each time point) in a 96-well plate (in duplicate) and incubated at +37 °C under gentle agitation for up to 3 h. At time 0 and afterward at the prefixed time points of 30 min and 3 h, two aliquots were transferred and three volumes of acetonitrile were added for protein precipitation, followed by centrifugation (4000 rpm, 15 min, 4 °C) and dilution with 0.1% HCOOH. Analysis by LC-ESI$^+$-MSMS using a fast gradient was performed using an API4000 triple quadrupole mass spectrometer (Applied Biosystems) in the multiple reaction monitoring mode (MRM). Results, as average of two replicates, were obtained by comparing the peak area at the different time points (30 min and 3 h) with that at time 0 and were reported as percentage remaining: percent remaining = $100 area_{STM}/area_{time\ 0}$ (where $area_{STM}$ is the MS peak area of the sample at the specific time points of 30 min and 3 h and $area_{time\ 0}$ is the MS area of the sample at time zero). Compounds were defined as stable, moderately unstable, or unstable based on the percent remaining: 80−100 stable, 50−80 moderately unstable, <50 unstable.

MDCK Cellular Permeability. Madin-Darby canine kidneys were maintained in tissue culture flasks in EMEM with Glutamax added with 1% MEM, penicillin (100 U/mL), streptomycin (100 ug/mL), and 10% FBS. Five days before the permeability experiment, the cells were split and placed on permeable cell culture inserts (24-well Millipore) at a density of 250 000 cells/well. Transepithelial electrical resistance (TEER) was measured for each well before incubation using an EVOMX instrument (WPI) to ensure that the monolayer was confluent and the tight junctions intact. A TEER > 70 Ohm × cm^2 was considered suitable for experimentation. Compounds (10 μM in HBSS-Hepes buffer) were added in duplicate to the donor chamber and buffer to the acceptor chamber (alternatively apical and basolateral) and incubated for 2 h at 37 °C under gentle agitation. Standards with a high (antipyrin), low (cimetidine), and medium (warfarin) permeability were incubated in the same plate under the same conditions. An aliquot (100 μL) from each well (both apical and basolateral) at time 0 and 120 min was filtered and analyzed by UPLC/TOF-MS. Following incubation, the cell monolayer was washed and incubated with Lucifer Yellow, a fluorescent probe with low permeability, to verify monolayer integrity after incubation. The UPLC separation was performed using a C-18 column (Acquity UPLC BEH C18, 1.7 μm, 2.1 mm × 50 mm, Waters). Samples were analyzed using an LTC premier TOF (Waters). The ESI positive W mode scan type was applied and the total ion current (TIC) scan range extended from 100 to 800 amu, with a scan time of 0.08 s. Acquisition was from 0.3 to 1.8 min. Quantitative data were automatically produced using the OpenLynx software. The apparent permeability (Papp) in centimeters per second was calculated using the following equation in both directions (apical-to-basolateral and basolateral-to-apical): $P_{app} = dC \times V_r/dt \times A \times C_0$ (where V_r was the volume (mL) of the receiver chamber, A was the surface area of the cell culture insert, and dt was the time in seconds). The mass balance in both directions was estimated by the following equation: mass balance = (final donor mass + mass transferred)/initial donor mass. The efflux ratio was calculated by comparing $P_{app\ B \to A}$ with $P_{app\ A \to B}$. A high efflux ratio was an indication of the compound being a substrate for efflux transporters. The alert threshold was an efflux ratio >3.

Electrophysiology. GH4C1cells stably expressing rat α7-nAChR were treated with 0.5 mM sodium butyrate added to the medium for two days before patch clamp recordings. Patch pipets had resistances of ~7 MΩ when filled with (in mM): 5 EGTA, 120 K-gluconate, 5 KCl, 10 HEPES, 5 K$_2$ATP, 5 Na$_2$-phosphocreatine, 1 CaCl$_2$, and 2 MgCl$_2$. Cells were voltage-clamped at −60 mV with a HEKA EPC-9 amplifier. To measure the fast activation and desensitization of the α7 current, the Dynaflow (Cellectricon) fast perfusion system with 16- or 48-well chips was used. Different concentrations of acetylcholine or **25** were applied to cells in between washes with bath solution (Hanks' Balanced Salt Solution +10 mM HEPES). Data were acquired at 1 kHz for 2 s episodes (500 ms bath, 500 ms agonist, 1000 ms wash) with a 10 s interval between episodes. Peak current amplitude and total charge (area under the curve) were measured with the HEKA Pulse program. Concentration−response curves and EC$_{50}$ values were plotted and calculated with Origin (MicroCal).

Radioligand Binding Assay. [^{3}H]-Epibatidine binding studies were performed as previously described.[35] Briefly, cell membrane preparations derived from GH4C1 cells stably expressing rat α7 nAChRs were suspended in binding buffer (50 mM HEPES, pH 7.4, 3 mM KCl, 70 mM NaCl, 10 mM MgCl$_2$), 5 nM [^{3}H]-epibatidine (GE Healthcare; SA = 53 Ci/mmol), and **25** to achieve a final volume of 200 μL in a 96-well polypropylene plate. Nicotine at 300 μM was used for determination of nonspecific binding. Following incubation at room temperature (23 °C) for 1 h, samples were rapidly filtered through Unifilter GF/B filters using a Filtermate (Perkin-Elmer) and washed five times with ice-cold binding buffer. Samples were processed and counted for radioactivity using a TopCount NXT (Perkin- Elmer). Competition binding curves were fitted with a four parameter logistic model. K_i values were calculated by the Cheng-Prusoff equation using the GraphPad Prism software package.

Receptor Selectivity and hERG Activity. Interaction of **25** with ~70 binding sites including all major classes of neurotransmitter, growth factor, and peptide receptors (Novascreen, Caliper Biosciences, HopkintonMA) was examined at 10 μM concentration. Activity at the hERG ion channel was determined by employing CHO cells stably expressing the channel and an IonWorks recording system.

Pharmacokinetics. Long Evans rats (age of 6−8 weeks, body weight 250−550 g) were administered compound **25** as a single dose of 20 mg/kg po (10 mg/kg po, for the brain study) at time 0 as a solution in 2% Tween, 0.5% methocell in water (volume 2.5 mL/kg). Levels in plasma were determined over a time period of 6 h in the po study and in brain at 0, 0.5, 1, and 3 h. The concentration of **25** in rat brain and plasma was measured by high performance liquid chromatography in combination with mass spectrometry (LC-MS/MS) with a limit of detection of 1 ng/mL in plasma and 3 ng/g in brain. Plasma samples were prepared by protein precipitation with acetonitrile containing 250 ng/mL of internal standard, centrifugation, and analysis of the supernatant by LC-MS/MS. Brain samples were prepared by homogenization and extraction with methanol. The homogenates were subsequently centrifuged, and the supernatant was analyzed by LC-MS/MS. Quantification was performed in a similar manner to that for the plasma samples.

Novel Object Recognition (NOR) Test. Male Long Evans rats (275−250 g; Charles River Laboratories) were individually housed with ad lib access to food and water and provided with nestlets for environmental enrichment. All habituation, training, and testing were performed under low illumination (approximately 10 l×) in a circular arena (70 cm diameter, 30 cm height) constructed of plastic surrounded by a black mesh curtain and containing corncob bedding. The NOR task was composed of three sessions: habituation, a sample trial (T1), and a choice trial (T2). Animal performance was tracked by video using Noldus Ethovision XT software (Noldus Information Technology, Inc., Leesburg, VA). Objects, constructed with Duplo (Lego, Billund, Denmark) were placed on the arena floor in one of four locations spaced evenly around the field approximately 10 cm from the field's edge. Rats were habituated to the arena, which contained two identical yellow cubes for a period of 15 min 1 day prior

to the T1 and T2 sessions. T2 consisted of a 5 min exploration of the field containing both a familiar object, previously explored in T1, and a novel object. The location of the objects, counterbalanced across treatment groups, remained constant for each animal during the habituation and the T1 and T2 trials. To evaluate the effect of **25** in the time delay deficit model of NOR, T2 was carried out 48 h after T1, and animals were treated with vehicle or **25** (0.3–10 mg/kg, po) 60 min prior to T1 ($N = 10$ per treatment group). Tolerance was assessed in rats treated chronically with compound **25** (10 mg/kg ip per day for 14 days) prior to the experiment. The effect of treatment on object exploration during the sample trial was examined using a one-way ANOVA on total contact time followed by Fisher's LSD group mean pairwise comparisons. The amount of time exploring the novel and familiar objects across treatment groups was analyzed using repeated measures ANOVA followed by Fisher's LSD post hoc.

Antagonism of MK-801 Induced Prepulse Inhibition (PPI) Deficits in Rats. Each testing chamber (SR-LAB system, San Diego Instruments, San Diego, CA) consisted of a Plexiglas cylinder (8.8 cm in diameter) mounted on a frame and held in position by four metal pins to a base unit. Movement of the subjects (male Long Evans rats, 200–300 g; Charles River Laboratories $n = 8$ per treatment group) within the cylinder was detected by a piezoelectric accelerometer attached below the frame. A loudspeaker mounted 24 cm above the cylinder provided background white noise, acoustic noise bursts, and acoustic prepulses. The entire apparatus was housed in a ventilated enclosure (39 cm × 38 cm × 56 cm). Presentation of acoustic pulse and prepulse stimuli was controlled by the SR-LAB software and interface system, which also digitized, rectified, and recorded the responses from the accelerometer. Mean startle amplitude was determined by averaging 100, 1 ms readings taken from the beginning of the pulse stimulus onset. For calibration purposes, sound levels were measured with a Quest sound level meter, scale "A", with the microphone placed inside the Plexiglas cylinder. Test sessions consisted of 61 total trials with a 15 s intertrial interval. Following a 5 min acclimation to a 64 dB background noise, four trial types (20 ms 120 dBpulse, or a 69, 74, or 79 dB 20 ms prepulse paired with a 120 dB 20 ms pulse, occurring 100 ms later onset to onset) were presented in a pseudorandom order. Compound **25** (3–30 mg/kg) was administered orally at 60 min prior to testing with MK-801 (0.085 mg/kg) administered sc 10 min prior to testing. Prepulse inhibition was defined as 100 − 100(startle amplitude on prepulse trials/startle amplitude on pulse alone trials). Data from the pulse-alone trials and average PPI values were analyzed using one-way ANOVA followed by a least significant difference post hoc test ($p < 0.05$).

4. Modeling Studies. All molecular modeling studies were performed on a DELL PowerEdge server equipped with four processors, Intel Xeon CPU 3.00 GHz. A homology model of the EC domain of nAChR was built by modeling the human $\alpha 7$ sequence for $\alpha 7$ nAChR on a 1UW6 PDB structure as a template. The amino acid numbering reported in the text refers to the 1UW6 sequence. The model was then used for docking purposes. Compound structures were modeled within the Maestro software suite (Maestro version 9.0; Schrodinger, LLC, New York). In particular, ligands were protonated at pH 7.4 and their geometries optimized using the LigPrep module (LigPrep 2.3; Schrodinger, LLC, New York). Docking into the orthosteric binding site of the homology model was performed by the docking program GOLD version 3.0.[39] Ligands were docked using default accurate genetic algorithm settings and the GOLDSCORE fitness function. The goodness of the docked poses was mainly evaluated via visual inspection and supported by the scoring value. Key pharmacophoric interaction between protonated nitrogen on the ligand and the backbone carbonyl of W143 was considered as a fundamental requisite to validate docking poses.

■ AUTHOR INFORMATION

Corresponding Author
*Phone: (+39) 0577381474. Fax: (+39) 0577381323. E-mail: riccardozanaletti@hotmail.com.

■ ABBREVIATIONS USED

ACh, acetylcholine; AChBP, acetylcholine binding protein; AD, Alzheimer's disease; BFC, 7-benzyloxy-4-trifluoromethylcoumarin; ACN, acetonitrile; B/P, brain to plasma ratio; CHO, Chinese hamster ovary; CREB, cAMP response element-binding; ESI, electrospray ionization; FLIPR, fluorescence imaging plate reader; HBSS, Hank's balanced salt solution; HEK, human embryo kidney; hERG, human ether-a-go-gorelated gene; HPLC, high pressure liquid chromatography; HRMS, high resolution mass spectrometry; LTQ, linear trap quadrupole; MDCK, Madin Darby canine kidney; MFC, 7-methoxy-4-trifluoromethylcoumarin; MPSA, molecular polar surface area; MS, mass spectrometry; NMDA, *N*-methyl-D-aspartate; NOR, novel object recognition; P450, cytochrome P450; PAMPA, parallel artificial membrane permeability assay; PDA, photodiode array; PPI, prepulse inhibition; Rt, retention time; SAR, structure−activity relationship; TLC, thin layer chromatography; TOF, time-of-flight; UPLC, ultraperformance liquid chromatography

■ REFERENCES

(1) Van Os, J.; Kapur, S. Schizophrenia. *Lancet* **2009**, *374*, 635−645.
(2) Brookmeyer, R.; Gray, S.; Kawas, C. Projections of Alzheimer's disease in the United States and the public health impact of delaying disease onset. *Am. J. Public Health* **1998**, *9*, 1337−1342.
(3) Brookmeyer, R.; Johnson, E.; Ziegler-Graham, K.; Arrighi, H. M. Forecasting the global burden of Alzheimer's disease. *Alzheimer's Dementia* **2007**, *3*, 186−191.
(4) Dani, J. A.; Bertrand, D. Nicotinic acetylcholine receptors and nicotinic cholinergic mechanisms of the central nervous system. *Annu. Rev. Pharmacol. Toxicol.* **2007**, *47*, 699−729.
(5) Albuquerque, E. X.; Pereira, E. F.; Alkondon, M.; Rogers, S. W. Mammalian nicotinic acetylcholine receptors: from structure to function. *Physiol. Rev.* **2009**, *89*, 73−120.
(6) Berg, D. K.; Conroy, W. G. Nicotinic alpha7 receptors: Synaptic options and downstream signaling in neurons. *J. Neurobiol.* **2002**, *53*, 512−523.
(7) Dajas-Bailador, F.; Wonnacott, S. Nicotinic acetylcholine receptors and the regulation of neuronal signalling. *Trends Pharmacol. Sci.* **2004**, *25*, 317−324.
(8) Adams, J.; Sweatt, J. Molecular psychology: Roles for the ERK MAP kinase cascade in memory. *Annu. Rev. Pharmacol. Toxicol.* **2002**, *42*, 135−163.
(9) Lindstrom, J. Neuronal nicotinic acetylcholine receptors. *Ion Channels* **1996**, *4*, 377−450.
(10) Newhouse, P.; Singh, A.; Potter, A. Nicotine and Nicotinic Receptor Involvement in Neuropsychiatric Disorders. *Curr. Top. Med. Chem.* **2004**, *4*, 267−282.
(11) Taly, A.; Corringer, P.-J.; Guedin, D.; Lestage, P.; Changeux, J.-P. Nicotinic receptors: allosteric transitions and therapeutic targets in the nervous system. *Nat. Rev. Drug Discovery* **2009**, *8*, 733−750.
(12) Decker, M. W.; Gopalakrishnan, M.; Meyer, M. D. The potential of neuronal nicotinic acetylcholine receptor agonists for treating CNS conditions. *Expert Opin. Drug Discovery* **2008**, *3*, 1027−1040.
(13) Gotti, C.; Riganti, L.; Vailati, S.; Clementi, F. Brain Neuronal Nicotinic Receptors as New Targets for Drug Discovery. *Curr. Pharm. Des.* **2006**, *12*, 407−428.
(14) Acker, B. A.; Jacobsen, E. J.; Rogers, B. N.; Wishka, D. G.; Reitz, S. C.; Piotrowski, D. W.; Myers, J. K.; Wolfe, M. L.; Groppi, V. E.;

Thornburgh, B. A.; Tinholt, P. M.; Walters, R. R.; Olson, B. A.; Fitzgerald, L.; Staton, T. J.; Raub, T. J.; Krause, M.; Li, K. S.; Hoffman, W. E.; Hajos, M.; Hurst, R. S.; Walker, D. P. Discovery of N-[(3R,5R)-1-azabicyclo[3.2.1]oct-3-yl]furo[2,3-c]pyridine-5-carboxamide as an agonist of the alpha7 nicotinic acetylcholine receptor: in vitro and in vivo activity. *Bioorg. Med. Chem. Lett.* **2008**, *18*, 3611−3615.

(15) Pichat, P.; Bergis, O. E.; Terranova, J.-P.; Urani, A.; Duarte, C.; Santucci, V.; Gueudet, C.; Voltz, C.; Steinberg, R.; Stemmelin, J.; Oury-Donat, F.; Avenet, P.; Griebel, G.; Scatton, B. SSR180711, a novel selective alpha7 nicotinic receptor partial agonist: (II) efficacy in experimental models predictive of activity against cognitive symptoms of schizophrenia. *Neuropsychopharmacology* **2007**, *32*, 17−34.

(16) Lippiello, P. M.; Bencherif, M.; Hauser, T. A.; Jordan, K. G.; Letchworth, S. R.; Mazurov, A. A. Nicotinic receptors as targets for therapeutic discovery. *Expert Opin. Drug Discovery* **2007**, *2*, 1185−1203.

(17) Freedman, R.; Adams, C. E.; Leonard, S. The alpha7-nicotinic acetylcholine receptor and the pathology of hippocampal interneurons in schizophrenia. *J. Chem. Neuroanat.* **2000**, *20*, 299−306.

(18) Kem, W. R. The brain alpha7 nicotinic receptor may be an important therapeutic target for the treatment of Alzheimer's disease: studies with DMXBA (GTS-21). *Behav. Brain Res.* **2000**, *113*, 169−181.

(19) Mazurov, A. A.; Speake, J. D.; Yohannes, D. Discovery and Development of α7 Nicotinic Acetylcholine Receptor Modulators. *J. Med. Chem.* **2011**, *54*, 7943−7961.

(20) Beers, W. H.; Reich, E. Structure and activity of acetylcholine. *Nature* **1970**, *228*, 917−922.

(21) Glennon, R. A.; Dukat, M. Central nicotinic receptor ligands and pharmacophores. *Pharm. Acta Helv.* **2000**, *74*, 103−114.

(22) Brejc, K.; van Dijk, W. J.; Klaassen, R. V.; Schuurmans, M.; van Der Oost, J.; Smit, A. B.; Sixma, T. K. Crystal structure of an ACh-binding protein reveals the ligand-binding domain of nicotinic receptors. *Nature* **2001**, *411*, 269−276.

(23) Celie, P. H.; van Rossum-Fikkert, S. E.; van Dijk, W. J.; Brejc, K.; Smit, A. B.; Sixma, T. K. Nicotine and carbamylcholine binding to nicotinic acetylcholine receptors as studied in AChBP crystal structures. *Neuron* **2004**, *41*, 907−914.

(24) Haydar, S. N.; Ghiron, C.; Bettinetti, L.; Bothmann, H.; Comery, T. A.; Dunlop, J.; La Rosa, S.; Micco, I.; Pollastrini, M.; Quinn, J.; Roncarati, R.; Scali, C.; Valacchi, M.; Varrone, M.; Zanaletti, R. SAR and biological evaluation of SEN12333/WAY-317538: novel alpha 7 nicotinic acetylcholine receptor agonist. *Bioorg. Med. Chem.* **2009**, *17*, 5247−5258.

(25) Ghiron, C.; Haydar, S. N.; Aschmies, S.; Bothmann, H.; Castaldo, C.; Cocconcelli, G.; Comery, T. A.; Di, L.; Dunlop, J.; Lock, T.; Kramer, A.; Kowal, D.; Jow, F.; Grauer, S.; Harrison, B.; La Rosa, S.; Maccari, L.; Marquis, K. L.; Micco, I.; Nencini, A.; Quinn, J.; Robichaud, A. J.; Roncarati, R.; Scali, C.; Terstappen, G. C.; Turlizzi, E.; Valacchi, M.; Varrone, M.; Zanaletti, R.; Zanelli, U. Novel alpha-7 nicotinic acetylcholine receptor agonists containing a urea moiety: identification and characterization of the potent, selective, and orally efficacious agonist 1-[6-(4-fluorophenyl)pyridin-3-yl]-3-(4-piperidin-1-ylbutyl) urea (SEN34625/WYE-103914). *J. Med. Chem.* **2010**, *53*, 4379−4389.

(26) Edink, E.; Rucktooa, P.; Retra, K.; Akdemir, A.; Nahar, T.; Zuiderveld, O.; van Elk, R.; Janssen, E.; van Nierop, P.; van Muijlwijk-Koezen, J.; Smit, A. B.; Sixma, T. K.; Leurs, R.; de Esch, I. J. Fragment Growing Induces Conformational Changes in Acetylcholine-Binding Protein: A Structural and Thermodynamic Analysis. *J. Am. Chem. Soc.* **2011**, *133*, 5363−5371.

(27) Bordwell, F. G.; Singer, D. L.; Satish, A. V. Effects of structural changes on acidities and homolytic bond dissociation energies of the nitrogen-hydrogen bonds in pyridones and related heterocycles. *J. Am. Chem. Soc.* **1988**, *110*, 2964−2968.

(28) Wishka, D. G.; Walker, D. P.; Yates, K. M.; Reitz, S. C.; Jia, S.; Myers, J. K.; Olson, K. L.; Jacobsen, E. J.; Wolfe, M. L.; Groppi, V. E.; Hanchar, A. J.; Thornburgh, B. A.; Cortes-Burgos, L. A.; Wong, E. H.; Staton, B. A.; Raub, T. J.; Higdon, N. R.; Wall, T. M.; Hurst, R. S.;

Walters, R. R.; Hoffman, W. E.; Hajos, M.; Franklin, S.; Carey, G.; Gold, L. H.; Cook, K. K.; Sands, S. B.; Zhao, S. X.; Soglia, J. R.; Kalgutkar, A. S.; Arneric, S. P.; Rogers, B. N. *J. Med. Chem.* **2006**, *49*, 4425−4436.

(29) Prickaerts, J.; Van Goethem, N. P.; Chesworth, R.; Shapiro, G.; Boess, F. G.; Methfessel, C.; Reneerkens, O. A. H.; Flood, D. G.; Hilt, D.; Gawryl, M.; Bertrand, S.; Bertrand, D.; König, G. EVP-6124, a novel and selective α7 nicotinic acetylcholine receptor partial agonist, improves memory performance by potentiating the acetylcholine response of α7 nicotinic acetylcholine receptors. *Neuropharmacology* **2011**, *2*, 1099−1110.

(30) Seneci, P.; Nicola, M.; Inglesi, M.; Vanotti, E.; Resnati, G. Synthesis of mono- and disubstituted 1H-imidazo [1,2-b] pyrazoles. *Synth. Commun.* **1999**, *29*, 311−341.

(31) Larsen, S. D.; Spilman, C. H.; Charles, H.; Bell, F. P.; Dinh, D. M.; Martinborough, E.; Wilson, G. J. Synthesis and hypocholesterolemic activity of 6,7-dihydro-4H-pyrazolo[1,5-a]pyrrolo[3,4-d]-pyrimidine-5,8-diones, novel inhibitors of acylCoA: cholesterol O-acyltransferase. *J. Med. Chem.* **1991**, *34*, 1721−1727.

(32) Suryakiran, N.; Reddy, T. S.; Latha, K.; Asha; Prabhakar, P.; Yadagiri, K.; Venkateswarlu, Y. An expeditious synthesis of 3-amino 2H-pyrazoles promoted by methanesulfonic acid under solvent and solvent-free conditions. *J. Mol. Catal., A: Chem.* **2006**, *258*, 371−375.

(33) O'Donnell, C. J.; Rogers, B. N.; Bronk, B. S.; Bryce, D. K.; Coe, J. W.; Cook, K. K.; Duplantier, A. J.; Evrard, E.; Haj_os, M.; Hoffmann, W. E.; Hurst, R. S.; Maklad, N.; Mather, R. J.; McLean, S.; Nedza, F. M.; O'Neill, B. T.; Peng, L.; Qian, W.; Rottas, M. M.; Sands, S. B.; Schmidt, A. W.; Shrikhande, A. V.; Spracklin, D. K.; Wong, D. F.; Zhang, A.; Zhang, L. Discovery of 4-(5-methyloxazolo[4,5-b]pyridin-2-yl)-1,4- diazabicyclo[3.2.2]nonane (CP-810,123), a novel α7 nicotinic acetylcholine receptor agonist for the treatment of cognitive disorders in schizophrenia: synthesis, SAR development, and in vivo efficacy in cognition models. *J. Med. Chem.* **2010**, *53*, 1222−1237.

(34) Still, W. C.; Kahn, M.; Mitra, A. J. Rapid chromatographic technique for preparative separations with moderate resolution. *J. Org. Chem.* **1978**, *43*, 2923−2925.

(35) Dunlop, J.; Roncarati, R.; Jow, B.; Bothmann, H.; Lock, T.; Kowal, D.; Bowlby, M.; Terstappen, G. C. In vitro screening strategies for nicotinic receptor ligands. *Biochem. Pharmacol.* **2007**, *74*, 1172−1181.

(36) Di, L.; Kerns, E.; Li, S.; Carter, G. Comparison of cytochrome P450 inhibition assays for drug discovery using human liver microsomes with LC-MS, rhCYP450 isozymes with fluorescence, and double cocktail with LC-MS. *Int. J. Pharm.* **2007**, *335*, 1−11.

(37) Crespi, C. L.; Miller, V. P.; Penman, B. W. Microtiter Plate Assays for Inhibition of Human, Drug-Metabolizing Cytochromes P450. *Anal. Biochem.* **1997**, *248*, 188−190.

(38) Palm, K.; Luthman, K.; Ros, J.; Grasjö, J.; Artursson, P. Effect of Molecular Charge on Intestinal Epithelial Drug Transport: pH Dependent Transport of Cationic Drugs. *J. Pharmacol. Exp. Ther.* **1999**, *291*, 435−443.

(39) Jones, G.; Willett, P.; Glen, R. C.; Leach, A. R.; Taylor, R. Development and Validation of a Genetic Algorithm for Flexible Docking. *J. Mol. Biol.* **1997**, *267*, 727−748.

(40) Di, L.; Kerns, E.; Fan, K.; McConnell, O. J.; Carter, G. T. High throughput artificial membrane permeability assay for bloodbrain barrier. *Eur. J. Med. Chem.* **2003**, *38*, 223−232.